Inorganic Chemistry

Article

pubs.acs.org/IC

Di- and Tetra-Nuclear Copper(II), Nickel(II), and Cobalt(II) Complexes of Four Bis-Tetradentate Triazole-Based Ligands: Synthesis, Structure, and Magnetic Properties

Juan Olguín,[†] Marguerite Kalisz,[‡,§] Rodolphe Clérac,[‡,§] and Sally Brooker*[,†]

[†]Department of Chemistry and MacDiarmid Institute for Advanced Materials and Nanotechnology, University of Otago, P.O. Box 56, Dunedin 9054, New Zealand

[‡]CNRS, CRPP, UPR 8641, F-33600 Pessac, France

[§]Univ. Bordeaux, CRPP, UPR 8641, F-33600 Pessac, France

Supporting Information

ABSTRACT: Four bis-tetradentate N^4-*substituted*-3,5-{bis-[bis-*N*-(2-pyridinemethyl)]aminomethyl}-4*H*-1,2,4-triazole ligands, L^{Tz1}–L^{Tz4}, differing only in the triazole N^4 substituent R (where R is amino, pyrrolyl, phenyl, or 4-*tert*butylphenyl, respectively) have been synthesized, characterized, and reacted with $M^{II}(BF_4)_2{\cdot}6H_2O$ (M^{II} = Cu, Ni or Co) and $Co(SCN)_2$. Experiments using all 16 possible combinations of metal salt and L^{TzR} were carried out: 14 pure complexes were obtained, 11 of which are *dinuclear*, while the other three are *tetranuclear*. The dinuclear complexes include two copper(II) complexes, $[Cu^{II}_2(L^{Tz2})(H_2O)_4](BF_4)_4$ (**2**), $[Cu^{II}_2(L^{Tz4})(BF_4)_2](BF_4)_2$ (**4**); two nickel(II) complexes, $[Ni^{II}_2(L^{Tz1})(H_2O)_3(CH_3CN)](BF_4)_4{\cdot}0.5(CH_3CN)$ (**5**) and $[Ni^{II}_2(L^{Tz4})(H_2O)_4](BF_4)_4{\cdot}H_2O$ (**8**); and seven cobalt(II) complexes, $[Co^{II}_2(L^{Tz1})(\mu\text{-}BF_4)](BF_4)_3{\cdot}H_2O$ (**9**), $[Co^{II}_2(L^{Tz2})(\mu\text{-}BF_4)](BF_4)_3{\cdot}2H_2O$ (**10**), $[Co^{II}_2(L^{Tz3})(H_2O)_2](BF_4)_4$ (**11**), $[Co^{II}_2(L^{Tz4})(\mu\text{-}BF_4)](BF_4)_3{\cdot}3H_2O$ (**12**), $[Co^{II}_2(L^{Tz1})(SCN)_4]{\cdot}3H_2O$ (**13**), $[Co^{II}_2(L^{Tz2})(SCN)_4]{\cdot}2H_2O$ (**14**), and $[Co^{II}_2(L^{Tz3})(SCN)_4]{\cdot}H_2O$ (**15**). The tetranuclear complexes are $[Cu^{II}_4(L^{Tz1})_2(H_2O)_2(BF_4)_2](BF_4)_6$ (**1**), $[Cu^{II}_4(L^{Tz3})_2(H_2O)_2(\mu\text{-}F)_2](BF_4)_6{\cdot}0.5H_2O$ (**3**), and $[Ni^{II}_4(L^{Tz3})_2(H_2O)_4(\mu\text{-}F_2)](BF_4)_6{\cdot}6.5H_2O$ (**7**). Single crystal X-ray structure determinations revealed different solvent content from that found by microanalysis of the bulk sample after drying under a vacuum and confirmed that **5′**, **8′**, **9′**, **11′**, **12′**, and **15′** are dinuclear while **1′** and **7′** are tetranuclear. As expected, magnetic measurements showed that weak antiferromagnetic intracomplex interactions are present in **1**, **2**, **4**, **7**, and **8**, stabilizing a singlet spin ground state. All seven of the dinuclear cobalt(II) complexes, **9**–**15**, have similar magnetic behavior and remain in the [HS–HS] state between 300 and 1.8 K.

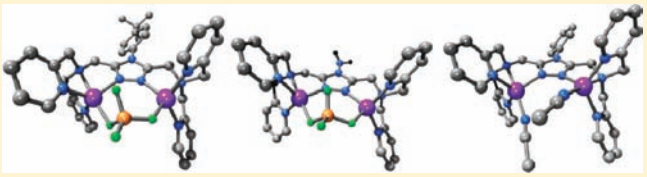

INTRODUCTION

Dinuclear complexes can be used as bioinorganic models, to gain understanding of the mechanism of complex biological systems (e.g., metalloenzymes) or to reproduce their catalytic activity.[1,2] They can also have interesting magnetic and/or electrochemical behavior due to the synergism between the metal centers.[3,4] Of the many nitrogen-containing heterocycles, diazines, diazoles, and triazoles are particularly well established as being able to facilitate the formation of dinuclear complexes bridged by the heterocycle. Of the di- and triazoles, pyrazole[4,5] and 1,2,4-1*H*-triazole[6−8] rings have been heavily used, as they can coordinate to two metal centers through adjacent nitrogen atoms, mediating magnetic and/or electrochemical communication and providing iron(II) with a ligand field that on occasions results in the observation of spin crossover (SCO) properties. Indeed, triazole-based ligands have been widely used to generate iron(II) SCO active systems, most of which are either monometallic or polymers. However, discrete polymetallic complexes, the simplest of which is dinuclear, may help us to understand the nature of the cooperativity during SCO; so they are of considerable current interest. The potentially *bis-bidentate* 3,5-bis(pyrid-2-yl)-N^4-substituted-4*H*-1,2,4-triazole (Rdpt) ligands have been used by many research groups (Figure 1); however, only in a few cases have dinuclear (doubly bridged) complexes been obtained (Figure 1).[7,8] It is now well established that the use of stoichiometric amounts of the reactants is not a guarantee of the formation of the desired nuclearity product.[9] Hence, we decided to increase the denticity of the triazole-based ligand and synthesized the *bis-terdentate* triazole ligand PMAT,[10] 3,5-bis{[*N*-(2-pyridinemethyl) amino]methyl}-4*H*-1,2,4-triazole (Figure 1), where the central triazole ring has been functionalized at the 3- and 5-positions with pyridine-based pendant arms. As expected, this conferred more predictability on the outcome of complexations, consistently giving dinuclear iron(II) complexes, including $[Fe^{II}_2(PMAT)_2](BF_4)_4{\cdot}DMF$, which undergoes an abrupt and complete "half" SCO, from [HS–HS] to [LS–HS], with $T_{1/2}$ = 240 K.[11−13]

Received: November 23, 2011
Published: April 6, 2012

   dx.doi.org/10.1021/ic202537c | *Inorg. Chem.* 2012, 51, 5058–5069

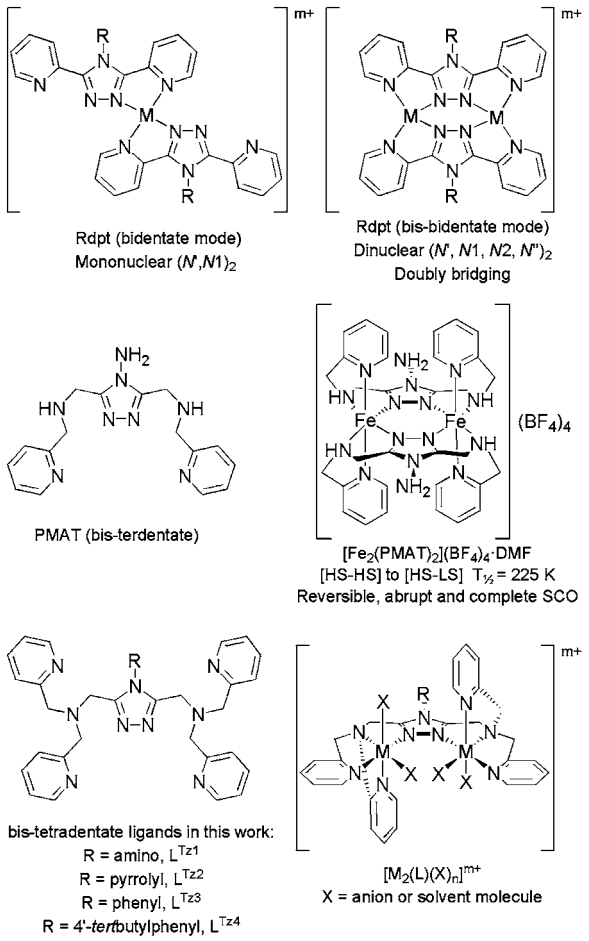

Figure 1. Top: Selected coordination modes observed in complexes of potentially bis-bidentate Rdpt. Middle: Literature bis-terdentate ligand PMAT and its dinuclear iron(II) SCO-active complex. Bottom: The bis-tetradentate ligands reported in this work and a schematic representation of the dinuclear complexes formed (only the *trans*-axial coordination mode is shown).

In the present work, we have further increased the denticity, moving to *bis-tetradentate* analogues, L^{TzR} (Figure 1). As for Rdpt and PMAT, the electronic and steric properties of this new ligand class can be tuned by changing the N^4 substituent. We decided to study the coordination chemistry of the ligands L^{Tz1} to L^{Tz4} with copper(II), nickel(II), and cobalt(II) to test whether they afford complexes of the type $[M_2L(X)_n]^{m+}$, where X is a solvent or anion (Figure 1). Dinuclear copper(II) and nickel(II) complexes were targeted due to the expected air stability and potential interest in them as inorganic models of metalloenzymes and/or as catalysts. Some cobalt(II) complexes are SCO-active;[14−18] hence, the cobalt(II) complexes of these ligands were also prepared, both as tetrafluoroborates and as thiocyanates.

RESULTS AND DISCUSSION

Synthesis of the Ligands. When we started this line of research, there were no examples in the literature of *bis-tetradentate* triazole-based ligands. However, in 2010, Yan and co-workers[19] described the synthesis of such a ligand, namely, 3,5-bis[bis(2-pyridylmethyl)aminomethyl]-N^4-amino-4*H*-1,2,4-triazole, L^{Tz1} (Figure 1). The authors did not give experimental details for the synthesis of L^{Tz1}, or spectroscopic characterization of it. Rather, they cited the synthesis of a pyridine-based analogue[20] (L^B, Figure S1), which, according to the original publication, was synthesized by stirring a suspension of 4-amino-3,5-bis(chloromethyl)-4*H*-1,2,4-pyridine and two equivalents of *N*-bis(2-pyridylethyl)amine with K_2CO_3 in acetonitrile at room temperature for 4 h. After filtration and solvent removal, L^B was obtained. No yield was reported.

The 3,5-bis(chloromethyl)-4-substituted-4*H*-1,2,4-triazole hydrochlorides used to generate the present ligands (L^{TzR}, Figure 2) were synthesized according to the protocols developed in this research group[10] for R = amino and pyrrolyl and by Sviridov and co-workers[21] for R = phenyl and *tert*-butylphenyl. One equivalent of the appropriate 3,5-bis(chloromethyl)-4-substituted-4*H*-1,2,4-triazole hydrochloride was then reacted with two equivalents of *N*-bis(2-pyridylmethyl)amine in the presence of an excess of potassium carbonate and a catalytic amount of potassium iodide in refluxing acetonitrile for 18 h. After workup, the ligands, L^{Tz1}–L^{Tz4}, were obtained as dark-brown oils in very good yields (76–96%). Interestingly, in all cases, these oils contain CH_2Cl_2, according to microanalysis and ^{1}H NMR spectral data, despite extensive drying under high-vacuum conditions for several days. This suggests that the CH_2Cl_2 may be hydrogen bonded to the ligands.

Synthesis of the Metal Complexes. As mentioned above there is only one example of a bis-tetradentate triazole-based ligand reported in the literature, L^{Tz1} (Figure 2). It was used to generate one complex, $[Cu^{II}_2(L^{Tz1})(\mu\text{-}SO_4)](PF_6)_2$, which promotes single and double strand DNA cleavage.[19]

All 14 of the complexes reported in this work were synthesized at room temperature, in the air, by reacting an acetonitrile solution of two equivalents of the metal salt, $M^{II}(BF_4)_2{\cdot}6H_2O$ (M^{II} = Cu, Ni, or Co) or $Co(SCN)_2$, with an acetonitrile solution of L^{Tz1}–L^{Tz4}. The reaction solutions were filtered and vapor diffused with diethyl ether. The resulting solids were filtered and dried under vacuum conditions. Experiments using all 16 possible combinations of metal salt and L^{TzR} were carried out: 14 pure complexes were obtained, 11 of which are believed to be *dinuclear* (Figure 1), while the other three are *tetranuclear* species.

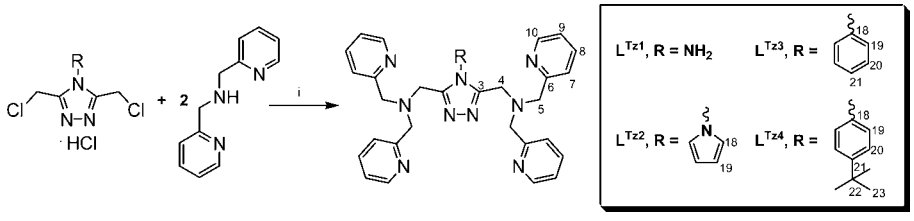

Figure 2. Synthesis and numbering scheme of the bis-tetradentate triazole-based ligands reported in this work. i: xs K_2CO_3, catalytic KI, CH_3CN, reflux.

dx.doi.org/10.1021/ic202537c | Inorg. Chem. 2012, 51, 5058−5069

Table 1. Selected Structural Parameters for the Complexes Presented in This Work

complex	M···M[b] [Å]	M−$N_{Triazole}$ [Å]	M−$(N-N)_{Triazole}$ [deg]	metal ion geometry	space group
$[Cu^{II}_4(L^{Tz1})_2(CH_3CN)_2(BF_4)_2](BF_4)_6\cdot CH_3CN$ (**1′**)	4.160(1)	2.155[a]	129.85[a]	octahedral[c] T^d = 0.83; trig. bipyr. τ^e = 0.60	$P\bar{1}$
$[Ni^{II}_2(L^{Tz1})(CH_3CN)_4](BF_4)_4\cdot 0.5(H_2O)\cdot 0.75(CH_3CN)$ (**5′**)	4.752(1)	2.115[a]	142.7[a]	octahedral	$Pna2_1$
$[Ni^{II}_4(L^{Tz3})_2(H_2O)_4(\mu\text{-}F)_2](BF_4)_6\cdot 4NO_2CH_3\cdot 2H_2O$ (**7′**)	4.541(1)[b]	2.060[a]	140.0[a]	octahedral	$P\bar{1}$
$[Ni^{II}_2(L^{Tz4})(CH_3CN)_4](BF_4)_4$ (**8′**)	4.693(1)	2.107(3)	141.7(2)	octahedral	$Fddd$
$[Co^{II}_2(L^{Tz1})(\mu\text{-}BF_4)](BF_4)_3\cdot 2CH_3CN$ (**9′**)	4.375(1)	2.052[a]	136.3[a]	trig. bipyr. τ^e = 0.90 and 0.93	$P\bar{1}$
$[Co^{II}_2(L^{Tz3})(CH_3CN)_2](BF_4)_4\cdot 0.5(C_4H_{10}O)\cdot 0.5H_2O$ (**11′**)	4.312(1)	2.048(5)	134.7(3)	trig. bipyr. τ^e = 0.92	$P2_12_12_1$
$[Co^{II}_2(L^{Tz4})(\mu\text{-}BF_4)](BF_4)_3\cdot CH_3CN$ (**12′**)	4.217(1)	2.042[a]	133.8[a]	trig. bipyr. τ^e = 0.76 and 0.79	$P2_1/n$
$[Co^{II}_2(L^{Tz3})(SCN)_4]$ (**15′**)	4.959(1)	2.234(3)	135.3(3)	octahedral Σ^f = 95.25°	$C2/c$

[a]Average value. [b]Distances between the metal centers bridged by the central triazole moiety. [c]Geometry of the copper(II) centers bound by the triazole ring nitrogen atoms. [d]As defined in refs 24−26. [e]As defined in ref 27. [f]As defined in refs 28−30.

In the case of copper(II) tetrafluoroborate, all four possible complexes were isolated, in 23−47% yields, as a blue solid for $[Cu^{II}_4(L^{Tz1})_2(H_2O)_2(BF_4)_2](BF_4)_6$ (**1**) and as green solids for $[Cu^{II}_2(L^{Tz2})(H_2O)_4](BF_4)_4$ (**2**), $[Cu^{II}_4(L^{Tz3})_2(H_2O)_2(\mu\text{-}F)_2](BF_4)_6\cdot 0.5H_2O$ (**3**), and $[Cu^{II}_2(L^{Tz4})(BF_4)_2](BF_4)_2$ (**4**). The proposed formulas are in agreement with the microanalysis results.

According to the microanalysis data and mass spectrometry results, three of the four possible nickel(II) complexes were successfully prepared, as brown solids in the case of the dinuclear complexes $[Ni^{II}_2(L^{Tz1})(H_2O)_3(CH_3CN)](BF_4)_4\cdot 0.5(CH_3CN)$ (**5**) and $[Ni^{II}_2(L^{Tz4})(H_2O)_4](BF_4)_4\cdot H_2O$ (**8**) and as a gray solid for $[Ni_4(L^{Tz3})_2(H_2O)_4(\mu\text{-}F_2)](BF_4)_6\cdot 6.5H_2O$ (**7**), in yields ranging from 17 to 55%. All attempts to synthesize the complex of L^{Tz2} (**6**), of the *N*-pyrrolyl substituted ligand, yielded a very hygroscopic oil.

Finally, seven of the eight possible cobalt(II) complexes were isolated. All seven are dinuclear, namely, $[Co^{II}_2(L^{Tz1})(\mu\text{-}BF_4)](BF_4)_3\cdot H_2O$ (**9**), $[Co^{II}_2(L^{Tz2})(\mu\text{-}BF_4)](BF_4)_3\cdot 2H_2O$ (**10**), $[Co^{II}_2(L^{Tz3})(H_2O)_2](BF_4)_4$ (**11**), $[Co^{II}_2(L^{Tz4})(\mu\text{-}BF_4)](BF_4)_3\cdot 3H_2O$ (**12**), $[Co^{II}_2(L^{Tz1})(SCN)_4]\cdot 3H_2O$ (**13**), $[Co^{II}_2(L^{Tz2})(SCN)_4]\cdot 2H_2O$ (**14**), and $[Co^{II}_2(L^{Tz3})(SCN)_4]\cdot H_2O$ (**15**). The tetrafluoroborate complexes were isolated as brown solids in 16−40% yields, while the thiocyanate complexes were obtained as dark green solids in 20−52% yields. Attempts to obtain the cobalt thiocyanate complex (**16**) of the *p-tert*-butylphenyl substituted ligand, L^{Tz4}, resulted in a very soluble complex which could not be cleanly isolated from the acetonitrile/diethyl ether mixture.

There are some important points to make regarding the three tetranuclear complexes. First, X-ray crystallography (see below) revealed that in $[Cu^{II}_4(L^{Tz1})_2(H_2O)_2(BF_4)_2](BF_4)_6$ (**1**) the NH_2 group (N^4-substitutent of the triazole) is coordinated to a copper(II) center. This is a very different coordination mode to that seen in **7′** (see later). This mode is unique to this complex as, (a) in this ligand, unlike the other ligands, the N^4-substituent contains a donor atom and (b) copper(II) binds amino donors quite well. Second, the other two tetranuclear complexes, namely, $[Cu^{II}_4(L^{Tz3})_2(H_2O)_2(\mu\text{-}F)_2](BF_4)_6\cdot 0.5H_2O$ (**3**) and $[Ni^{II}_4(L^{Tz3})_2(H_2O)_4(\mu\text{-}F)_2](BF_4)_6\cdot 6.5H_2O$ (**7**), were isolated after a second recrystallization of the initial product, from *nitromethane* by diethyl ether vapor diffusion. Third, X-ray crystallography (see below) shows that **7** is indeed a tetranuclear complex, featuring two doubly bridging fluoride ions. The hydrolysis of BF_4 anions and coordination of the resulting fluoride anion to the metal complex is not uncommon and has been described by other authors, including examples of dinuclear copper(II)[22] and cobalt(II)[23] pyrazolate-based analogues prepared in *methanol*. Interestingly, no methanol was employed in the present work, but water is ubiquitous. Crystals were not obtained for **3**, but as it was prepared in the same manner, and the microanalysis data are consistent with formulation as a tetranuclear complex with bridging fluoride ions, it is proposed that this compound is also tetranuclear. The electrospray ionization mass spectra for **3** and **7** showed only dinuclear fragments; however, (a) extensive fragmentation of our complexes in solution and/or in our spectrometer is commonplace and (b) while some of the fragments observed contain F^-, this is also true of some of the above *dinuclear* complexes (presumably due to decomposition of BF_4 in the spectrometer).

X-Ray Crystallography. All eight of the X-ray crystal structures presented in this section were acquired at low temperatures (89−90 K). A summary of some key structural parameters is presented in Table 1. Six of the structures are of dinuclear complexes, while the other two are of tetranuclear complexes. Unless otherwise stated, single crystals suitable for X-ray crystallography were obtained by diethyl ether vapor diffusion into an acetonitrile solution of the complex. It is important to note that the nature and content of the crystallization solvent identified in the X-ray crystal structure differs from that found by microanalysis after drying the sample. This commonly occurs in large complexes, with the solvent of crystallization that packs around the complexes in the crystals lost on drying, sometimes being replaced by atmospheric water.

Copper(II) Structure. The tetranuclear nature of **1′** was confirmed by X-ray crystallography (Figures 3 and 4, Tables 1 and S1). The solvent content differs from that found by microanalysis after drying under vacuum conditions; namely, the crystals are $[Cu^{II}_4(L^{Tz1})_2(CH_3CN)_2(BF_4)_2](BF_4)_6\cdot 6.3CH_3CN$ (**1′**). This complex crystallizes in the $P\bar{1}$ space group. The asymmetric unit comprises half of the complex cation, four BF_4 anions, two full occupancy, a 0.50 occupancy, and a 0.65 occupancy acetonitrile solvent molecule (Figure 3). The other half of the complex is generated by a center of inversion.

Interestingly, L^{Tz1} is bonded to the copper(II) centers in an asymmetric coordination mode that is different from that observed in the only related literature complex, $[Cu^{II}_2(L^{Tz1})(\mu\text{-}SO_4)](PF_6)_2$.[19] This results in two crystallographically independent copper(II) centers: Cu(1) is bound to N(1) of the triazole ring as expected, whereas Cu(2) is instead bound to

dx.doi.org/10.1021/ic202537c | Inorg. Chem. 2012, 51, 5058−5069

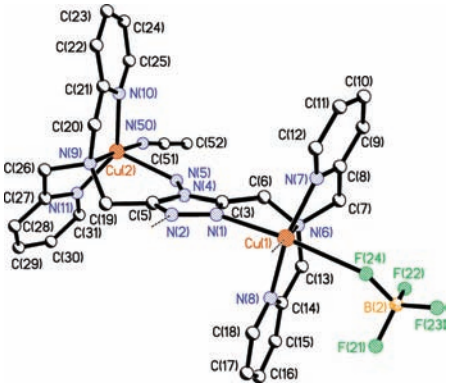

Figure 3. Ball and stick representation of the **asymmetric unit** of $[Cu^{II}_4(L^{Tz1})_2(CH_3CN)_2(BF_4)_2](BF_4)_6{\cdot}6.3CH_3CN$ (**1′**). Hydrogen atoms, and uncoordinated anion and solvent molecules, are omitted for the sake of clarity.

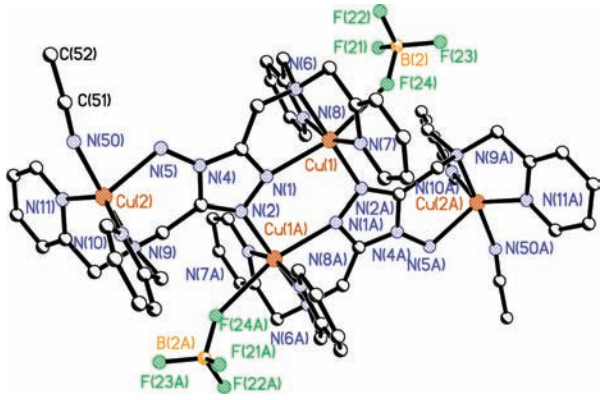

Figure 4. Ball and stick representation of $[Cu^{II}_4(L^{Tz1})_2(CH_3CN)_2(BF_4)_2](BF_4)_6{\cdot}6.3CH_3CN$ (**1′**), showing the complete tetranuclear unit. Hydrogen atoms, and uncoordinated anion and solvent molecules, are omitted for the sake of clarity.

the amino nitrogen atom out the "back" of the triazole ring (Figure 3). Overall, Cu(1) is six-coordinate, bound to N(1), the tertiary amine N(6), two pyridine rings of the pendant arms, N(7) and N(8), and to one fluorine atom of a BF_4 anion. The geometry is best described as distorted octahedral, axially elongated along N(1)−Cu(1)−F(24) due to the Jahn−Teller effect (Cu(1)−N(1) = 2.289(5) Å; Cu(1)−F(24) = 2.568(4) Å). In contrast, the shortest bond is Cu(1)−$N_{pyridine}$ (Cu(1)−N(7) = 1.985(5) Å). The pyridine rings coordinated to Cu(1) are almost at right angles to the triazole ring to which they are attached (N7 = 73.4(3), N8 = 83.3(3)°). Cu(1) lies out of the triazole ring plane, toward N(7), by 0.38(1) Å. The other copper(II) center, Cu(2), is five-coordinate. It coordinates to the tertiary amine, N(9), and the two pyridine rings of the pendant arm, N(9) and N(10), the primary amino group at the four position of the triazole ring, N(5), and an acetonitrile molecule, N(50) (Figure 3). The geometry of Cu(2) is best described as very distorted trigonal bipyramidal (τ = 0.60).[27] The longest bond to Cu(2) involves the amino group (N^4-susbtituent of the triazole ring, Cu(2)−N(5) = 2.231(6) Å), while the shortest involves the acetonitrile, Cu(2)−N(50) = 1.987(8) Å. This center, Cu(2), lies well out of the triazole plane (0.83(1) Å). The center of inversion generates the other half of the complex, forming a doubly triazole-bridged dinuclear fragment at the heart of this tetranuclear complex (Figure 4).

There are four independent Cu···Cu separations, namely Cu(1)···Cu(1A) = 4.160(1) Å, Cu(1)···Cu(2) = 6.300(1) Å, Cu(1A)···Cu(2) = 7.355(1) Å, and Cu(2)···Cu(2A) = 13.026(2) Å (A = 1 − x, 1 − y, 1 − z). The doubly triazole-bridged Cu(1)···Cu(1A) separation is similar to the 4.404 Å seen in the *dinuclear, singly* triazole-bridged literature complex $[Cu^{II}_2(L^{Tz1})(\mu\text{-}SO_4)](PF_6)_2$.[19] The moderate to strong anion−π and solvent−π interactions in **1′** are detailed in the Supporting Information.

Nickel(II) Structures. The dinuclear complexes $[Ni^{II}_2(L^{Tz1})(CH_3CN)_4](BF_4)_4{\cdot}0.5(H_2O){\cdot}0.75(CH_3CN)$ (**5′**) and, solvent free, $[Ni^{II}_2(L^{Tz4})(CH_3CN)_4](BF_4)_4$ (**8′**) crystallize in the space groups $Pna2_1$ (noncentrosymmetric; the entire complex is in the asymmetric unit) and F_{ddd} (centrosymmetric; the asymmetric unit comprises half the complex and two tetrafluoroborate anions; Figures 5 and S2, Tables 1 and S2). In

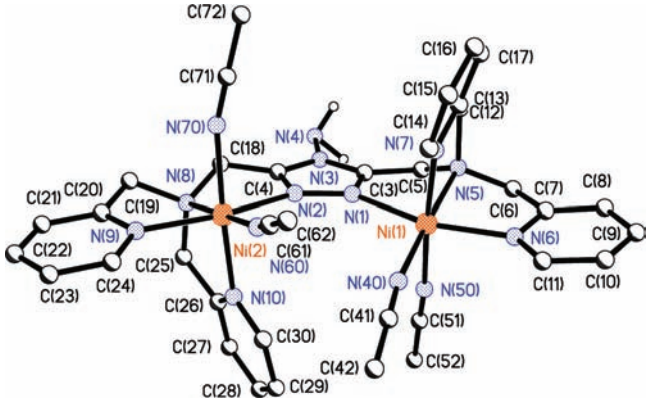

Figure 5. Ball and stick representation of $[Ni^{II}_2(L^{Tz1})(CH_3CN)_4]$-$(BF_4)_4{\cdot}0.5(H_2O){\cdot}0.75(CH_3CN)$ (**5′**). The solvent molecules of crystallization, hydrogen atoms, and anion molecules are omitted for the sake of clarity.

the latter complex, a 2-fold axis that runs through C(8) (*tert*-butyl group), C(7) and C(4) (phenyl group), and N(2) (triazole) generates the other half of the complex (Figure S2).

All of the nickel(II) centers are in distorted octahedral environments comprising one nitrogen donor of the central bridging triazole unit, all three donors from one pendant arm (a tertiary amine and two pyridines), and two cis-bound acetonitrile molecules (one is *trans* to the tertiary amine, while the other is *trans* to a pyridine ring). The bonding to the nickel(II) centers is very similar (Tables 1 and S2).

In all cases, the longest bond is Ni−N_{amine} (2.111(3)−2.132(4) Å), while the shortest involves either acetonitrile (2.025(3), 2.045(4) Å) or pyridine (2.044(4) Å). In the L^{Tz1} complex, Ni(1) is coplanar with the triazole while Ni(2) is 0.145(7) Å out of the triazole plane, whereas in the L^{Tz4} complex Ni(1) is only 0.090(7) Å out of plane. The Ni(1)···Ni(2) separation, 4.753(1) Å, is large in the L^{Tz1} complex, as can be expected given that this complex has the largest M−(N−N)$_{triazole}$ angle of any of these complexes (Table 1). This angle is smaller in the L^{Tz4} complex (Table 1), and in combination with the slightly shorter Ni−$N_{triazole}$ and more "in plane" location of the nickel(II) centers, this leads to a somewhat shorter Ni···Ni separation (4.541(1) Å). On each side of the triazole unit, one of the two pyridine rings is almost parallel to the bridging triazole ring (trz-py: L^{Tz1} N(6) = 9.0(2)°, N(9) = 8.2(2)°; L^{Tz4} N(4) = 7.1(3)°), whereas the other is almost perpendicular (trz-py: L^{Tz1} N(7) = 73.2(2)°,

dx.doi.org/10.1021/ic202537c | *Inorg. Chem.* 2012, 51, 5058−5069

N(10) = 84.7(2)°; L^{Tz4} N(5) = 82.1(1)°). The phenyl ring at the 4 position in the L^{Tz4} ligand is twirled around N2−C4 such that it is at 47.7(2)° to the attached triazole ring. In both cases, the axial pendant arms are coordinated in a *trans*-axial mode (one up and the other down with respect the central triazole bridge/equatorial plane).

Hydrogen bonding involving the $[Ni^{II}_2(L^{Tz1})(CH_3CN)_4]^{4+}$ cations, surrounding anions, and the solvent molecules is observed. A careful analysis of the crystal packing revealed that relatively strong anion−π interactions are a feature of both of these dinickel(II) structures. All of these interactions are detailed in the Supporting Information.

In an attempt to obtain crystals suitable for X-ray crystallography, the dinuclear product initially obtained (see the Experimental Section) from the 2:1 reaction of $Ni^{II}(BF_4)_2{\cdot}6H_2O$ with L^{Tz3} in acetonitrile was subsequently recrystallized from nitromethane by diethyl ether vapor diffusion. The X-ray structure determination revealed it to be the *tetranuclear* complex $[Ni^{II}_4(L^{Tz3})_2(H_2O)_4(\mu\text{-}F)_2](BF_4)_6{\cdot}4NO_2CH_3{\cdot}2H_2O$ (7′, Figures 6 and 7). It crystallizes

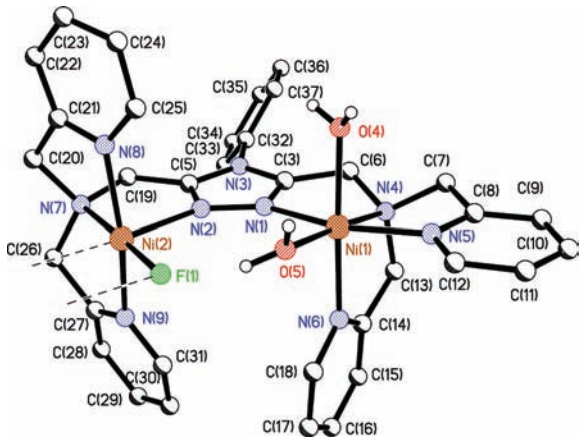

Figure 6. Ball and stick representation of the **asymmetric unit** of $[Ni^{II}_4(L^{Tz3})_2(H_2O)_4(\mu\text{-}F)_2](BF_4)_6{\cdot}4NO_2CH_3{\cdot}2H_2O$ (7′). The dotted lines represent the connection with the second half of the dimer. The hydrogen atoms except for those attached to the water molecules, and the uncoordinated solvent molecules and anions, are omitted for the sake of clarity.

in the $P\bar{1}$ space group. This complex can be viewed as a dimer of dinuclear units, held together by two bridging fluoride anions. These coordinated fluoride anions are presumably the result of hydrolysis of some of the BF_4 anions, something that can occur in the presence of metal ions.[22,23]

The asymmetric unit (Figure 6) comprises one bis-tetradentate triazole ligand, three tetrafluoroborate anions, and two nitromethane and one water molecule. The other half of the molecule is generated by a center of inversion (Figure 7).

The L^{Tz3} ligand provides a single N^1N^2 bridge between the two crystallographically independent nickel ions (Ni(1)···Ni(2) = 4.5413(9) Å; Ni(1) = 0.150(7) Å, Ni(2) = 0.040(7) Å out of the triazole plane), both of which are again octahedral (Tables 1 and S2). They have coordination spheres akin to those observed in the above dinuclear nickel complexes, but rather than two acetonitrile molecules, Ni(1) coordinates two water molecules and Ni(2) binds two fluoride anions that doubly bridge to the symmetry generated Ni(2A) center of a second dinuclear unit. The resulting Ni(2)···Ni(2A) separation is just 3.1234(9) Å (A = 1 − x, 2 − y, 1 − z; Figure 7). Once again,

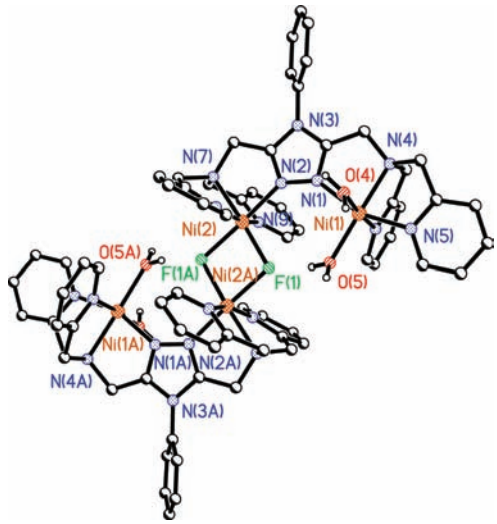

Figure 7. Ball and stick representation of $[Ni^{II}_4(L^{Tz3})_2(H_2O)_4(\mu\text{-}F)_2](BF_4)_6{\cdot}4NO_2CH_3{\cdot}2H_2O$ (7′). The hydrogen atoms except for those attached to the water molecules, and the uncoordinated solvent molecules and anions, are omitted for the sake of clarity.

the longest Ni−N bonds are to the tertiary amine (Ni(1)−N(4) = 2.126(3), Ni(2)−N(7) = 2.110(3) Å), whereas the shortest involve the pyridine ring that is almost parallel to the triazole ring (Ni(1)−N(5) = 2.039(4) Å; tz-py = 3.33°) and the fluoride atom (Ni(2)−F(1) = 2.033(2) Å). The other pyridine ring bound to Ni(1), N(6), is almost perpendicular to the triazole ring (86.00°). In contrast, *both* of the pyridine rings on the other pendant arm are approximately at right angles to the triazole ring (N(8) = 87.4(2)°; N(9) = 79.1(2)°). The phenyl ring at the 4 position of the triazole ring is twisted by 55.94° out of the triazole plane.

A detailed analysis of the crystal packing showed, once again, that the triazole moiety is "sandwiched" by π interactions, but in this case by a tetrafluoroborate anion and a nitromethane solvent molecule (see Supporting Information, Figure S15 and Table S13).

Interestingly, there are only three structurally characterized *dinuclear* nickel(II) complexes (CSD version 5.31, updated February 2010)[31,32] in which the metal centers are *doubly bridged by fluoride ligands* (Ni−$(\mu\text{-}F)_2$−Ni). One is an organometallic complex in which both nickel(II) centers are square planar.[33] The other two are a dimer of mononuclear nickel(II) complexes of a thioether-linked pyridine-based N_2S_2-donor macrocyclic ligand, $[Ni^{II}_2(MC)_2(\mu\text{-}F)_2](BF_4)_2$,[34] and a complex of an acyclic bis-bidentate pyrazole-based N_2-donor ligand, $[Ni^{II}_2(L_m)_2(\mu\text{-}F)_2](BF_4)_2$,[35] both of which feature octahedral nickel(II) centers (Supporting Information, Figure S5). In the latter two complexes, the Ni···Ni separations are 3.0863(6) vs 3.14 Å, the Ni−F bonds are 2.0041(13)/2.0169(13) vs 2.010(2)/2.015(2) Å, while the F−Ni−F and Ni−F−Ni bond angles are 79.73(5) vs 77.62° and 100.27(5) vs 102.4(1)°, respectively.[34,35] These are in reasonable agreement with the above results for our tetranuclear complex (Ni···Ni = 3.1234(9) Å; Ni−F = 2.033(2), 2.086(2) Å; F(1)−Ni(2)−F(1A) = 81.39(9)°, Ni(2)−F(1)−Ni(2A) = 98.6(1)°, A = x + 1, 2 − y, 1 − z). The slightly shorter Ni−F bonds, and hence Ni···Ni separation, in the macrocyclic complex are perhaps due to the intramolecular hydrogen bond formed between F(1) and the coordinated water molecule O(5) (Supporting Information, Figure S4).

dx.doi.org/10.1021/ic202537c | *Inorg. Chem.* 2012, 51, 5058−5069

Table 2. Selected Bond Lengths for the Complexes Presented in This Work

complex	M−$N_{triazole}$ range/average [Å]	M−N_{amine} range/average [Å]	M−$N_{pyridine}$ range/average [Å]
$[Cu^{II}_4(L^{Tz1})_2(CH_3CN)_2(BF_4)_2]_6\cdot 6.3CH_3CN$ (**1′**)	2.021(5)−2.289(5)/2.155	2.020(6)−2.069(5)/2.045	1.985(5)−2.020(6)/1.998
$[Ni^{II}_2(L^{Tz1})(CH_3CN)_4](BF_4)_4\cdot 0.5(H_2O)\cdot 0.75(CH_3CN)$ (**5′**)	2.111(4)−2.119(4)/2.115	2.120(4)−2.132(4)/2.126	2.044(4)−2.078(4)/2.064
$[Ni^{II}_4(L^{Tz3})_2(H_2O)_4(\mu\text{-}F)_2](BF_4)_6\cdot 4NO_2CH_3\cdot 2H_2O$ (**7′**)	2.040(3)−2.079(3)/2.060	2.093(3)−2.110(3)/2.102	2.039(4)−2.061(3)/2.050
$[Ni^{II}_2(L^{Tz4})(CH_3CN)_4](BF_4)_4$ (**8′**)	2.107(3)	2.111(3)	2.049(3)−2.082(3)/2.066
$[Co^{II}_2(L^{Tz1})(\mu\text{-}BF_4)](BF_4)_3\cdot 2CH_3CN$ (**9′**)	2.040(5)−2.062(5)/2.051	2.238(5)−2.251(6)/2.245	2.051(5)−2.064(5)/2.056
$[Co^{II}_2(L^{Tz3})(CH_3CN)_2](BF_4)_4\cdot 0.5(C_4H_{10}O)\cdot 0.5H_2O$ (**11′**)	2.048(5)	2.228(5)	2.030(5)−2.058(5)/2.044
$[Co^{II}_2(L^{Tz4})(\mu\text{-}BF_4)](BF_4)_3\cdot CH_3CN$ (**12′**)	2.037(3)−2.047(3)/2.042	2.215(3)−2.240(3)/2.228	2.044(3)−2.062(3)/2.053
$[Co^{II}_2(L^{Tz3})(SCN)_4]$ (**15′**)	2.234(4)	2.229(4)	2.104(4)− 2.142(4)/2.123

There are eight structurally characterized dinuclear octahedral nickel(II) complexes of bis-tetradentate *pyrazolate*-based ligands in the literature.[36−39] As expected, the Ni−$N_{pyrazolate}$ bonds are slightly shorter, due to the negatively charged nature of the pyrazolate ring, 1.943(4)−2.144(3) Å, than the Ni−$N_{triazole}$ bonds in the triazole complexes reported in this work, 2.040(3)−2.119(4) Å (Table 2). The Ni−N_{amine} and Ni−N_{py} bonds in the pyrazolate complexes (2.096(3)−2.205(1) and 2.043(3)−2.178(5) Å, respectively) are similar or slightly longer than in our triazole complexes (2.093(3)−2.132(4) and 2.039(4)−2.082(3) Å, respectively, Table 2). The Ni···Ni separations in the dinuclear octahedral literature complexes (4.092−4.684 Å, Supporting Information, Table S6) are mostly shorter than the range found in the complexes reported here (4.541−4.752 Å) due to the additional bridging ligand in the former complexes (e.g., Cl, N_3, or CH_3COO), bringing them closer together. There are no examples of *tetranuclear* nickel(II) complexes of these pyrazolate ligand analogues.

Cobalt(II) Structures. The cobalt(II) tetrafluoroborate complexes $[Co^{II}_2(L^{Tz1})(\mu\text{-}BF_4)](BF_4)_3\cdot 2CH_3CN$ (**9′**), $[Co^{II}_2(L^{Tz3})(CH_3CN)_2](BF_4)_4\cdot 0.5(C_4H_{10}O)\cdot 0.5H_2O$ (**11′**), and $[Co^{II}_2(L^{Tz4})(\mu\text{-}BF_4)](BF_4)_3\cdot CH_3CN$ (**12′**) crystallized in the $P\bar{1}$, $P2_12_12_1$ (noncentrosymmetric) and $P2_1/n$ space groups, respectively (Figures 8, 9, and S3; Tables 1 and S3). Only in the

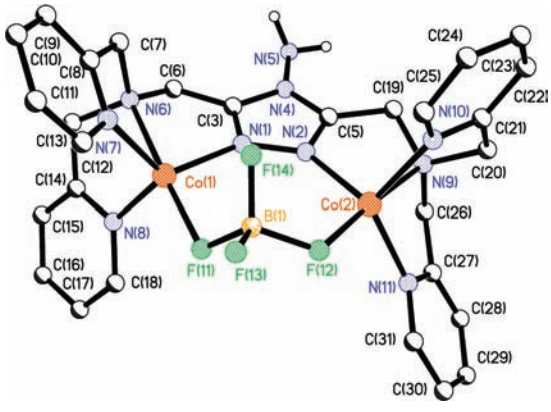

Figure 8. Ball and stick representation of $[Co^{II}_2(L^{Tz1})(\mu\text{-}BF_4)](BF_4)_3\cdot 2CH_3CN$ (**9′**). Hydrogen atoms, except for those on the amino group, solvent molecules and uncoordinated anions are omitted for the sake of clarity.

L^{Tz3} complex is internal symmetry present, generating the other half of the complex by a 2-fold axis that passes through the middle of the triazole and phenyl rings (N(4), C(32), C(35), Figure 9).

In all three structures, the cobalt(II) centers have a distorted trigonal pyramidal geometry (Table 1), and the three equatorial positions are occupied by nitrogen atoms from a triazole and

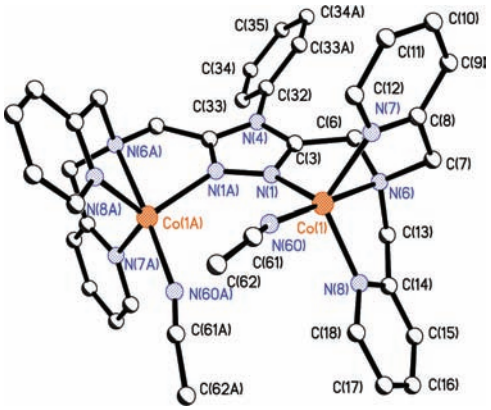

Figure 9. Ball and stick representation of $[Co^{II}_2(L^{Tz3})(CH_3CN)_2](BF_4)_4\cdot 0.5(C_4H_{10}O)\cdot 0.5(H_2O)$ (**11′**). Hydrogen atoms, C(72), uncoordinated solvent molecules, and anions are omitted for the sake of clarity. Symmetry operation used to generate equivalent atoms: A = $-x + 1, -y + 1, z$.

two pyridines of a pendant arm (Tables 1 and S3). For the L^{Tz3} complex, the apical positions are occupied by the acetonitrile ligand and by the tertiary amine nitrogen atom, whereas for the L^{Tz1} and L^{Tz4} complexes, the apical positions are occupied by the fluoride of the bridging tetrafluoroborate anion and the nitrogen of the tertiary amine. In both cases, the Co−F bond is the shortest bond (L^{Tz1}: Co(1)−F(11) = 2.024(4) Å, Co(2)−F(12) = 2.005(4) Å. L^{Tz4}: Co(1)−F(11) = 1.998(2) Å, Co(2)−F(12) = 1.992(3) Å, Table 2). In all of these structures, the longest Co−X bond consistently involves the tertiary amine (L^{Tz1}: Co(1)−N(6) = 2.238(4) Å, Co(2)−N(9) = 2.251(5) Å. L^{Tz3}: Co(1)−N(6) = 2.227(5) Å. L^{Tz4}: Co(1)−N(4) = 2.240(3) Å and Co(2)−N(7) = 2.215(3) Å, Table 2).

The Co···Co separations are 4.375(1), 4.312(1), and 4.217(1) Å, for the complexes of L^{Tz1}, L^{Tz3}, and L^{Tz4}, respectively; unsurprisingly, this distance decreases with decreasing M−(N−N)$_{triazole}$ angle (Table 1). The crystallographically unique cobalt center in the L^{Tz3} complex is 0.358(9) Å out of the plane defined by the triazole ring, whereas in the L^{Tz4} complex, it is out of the plane by only 0.151(5) and 0.226(5) Å. In the L^{Tz1} complex, one of the cobalt(II) centers is in plane while the other one is 0.358(9) Å out of the plane.

A detailed analysis of the packing interactions for these three dinuclear cobalt(II) complexes is presented in the Supporting Information. To the best of our knowledge, there is only one previous example of a tetrafluoroborate anion bridging two cobalt(II) centers, namely in the cage-type complex $[Co^{II}_2(L^{C})_4(CH_3CN)(\mu\text{-}BF_4)](BF_4)_3$ (Figure S7).[40] However, in that case, the BF_4 unit is coordinated to two already pentacoordinated metal centers (Co−F = 2.406(9) Å) with the cobalt(II) centers 7.069(3) Å apart.[40] This means that the

dx.doi.org/10.1021/ic202537c | *Inorg. Chem.* 2012, 51, 5058−5069

overall coordination sphere of the cobalt(II) in this known complex is hexacoordinate, and therefore the average Co−F distance is expected to be longer than those reported in the present work (2.015 and 1.995 Å) for the five coordinate cobalt(II) centers in $[Co^{II}_2(L^{Tz1})(\mu\text{-}BF_4)](BF_4)_3{\cdot}2CH_3CN$ (**9′**) and $[Co^{II}_2(L^{Tz4})(\mu\text{-}BF_4)](BF_4)_3{\cdot}CH_3CN$ (**12′**), as it is found to be. The longer Co−F bond lengths are consistent with the larger Co···Co separation seen in $[Co^{II}_2(L^{C})_4(CH_3CN)_2(\mu\text{-}BF_4)](BF_4)_3$.

There are 12 structurally characterized dinuclear cobalt(II) complexes of bis-tetradentate *pyrazolate* ligands in a penta-coordinate environment (see Supporting Information, Figure S8) found in the literature.[23,41−43] As expected, in these pyrazolate complexes, the $Co-N_{prazolate}$ bonds are shorter (1.944(1)−2.043(5) Å) than the $Co-N_{triazole}$ bonds found in the complexes reported here (2.037(3)−2.062(5) Å). The $Co-N_{amine}$ bonds are 1.945(4)−2.394(2) Å in the pyrazolate complexes, whereas in the triazole complexes, they are 2.111(3)−2.251(6) Å.

The complex $[Co^{II}_2(L^{Tz3})(SCN)_4]$ (**15′**) crystallizes in the *C*2/*c* space group. The asymmetric unit comprises half of the complex (Figure 10). The other half is generated by a 2-fold

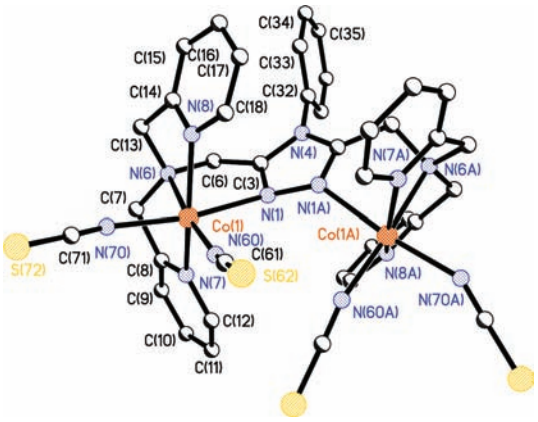

Figure 10. Ball and stick representation of $[Co^{II}_2(L^{Tz3})(SCN)_4]$ (**15′**). Hydrogen atoms are omitted for the sake of clarity. Symmetry operation to generate equivalent atoms: A = 1 − *x*, *y*, 0.5 − *z*.

axis that passes through the middle of the triazole (N(4)) and phenyl rings (C(32) and C(35)).

In this case, the coordination sphere of the cobalt(II) center is octahedral. Each metal center is coordinated to the tertiary amine, two pyridine nitrogen donors of the pendant arm, and the central bridging triazole ring. The last two positions are occupied by two thiocyanate anions coordinated through the nitrogen donors, cis to one another. The cobalt(II) centers are 0.911(5) Å out of the triazole plane and are 4.959(1) Å apart from one another. The degree of distortion from pure octahedral geometry is considerable, as evidenced by the distortion parameter Σ of 95.25°. The parameter Σ is the sum of the absolute values of the deviation from 90° of each of the 12 cis angles in the coordination sphere.[28−30]

According to the CSD, there is only one example of a dinuclear cobalt(II) complex that contains at least one triazole bridging moiety and both cobalt(II) centers coordinated to two thiocyanate anions, each with a N_6 coordination sphere, namely, $[Co^{II}_2(\mu\text{-PhTz})_3(PhTz)_2(SCN)_4]$, where PhTz = N^4-phenyl-1,2,4-1*H*-triazole.[44] In that triply triazole-bridged complex, the $Co-N_{NCS}$ distance averages 2.088 Å (range 2.0711(1)−2.1157(2) Å) while the $Co-N_{triazole}$ distance averages 2.152 Å (range 2.1414(2)−2.1685(2) Å). In the case of our dinuclear complex, the $Co-N_{NCS}$ bonds are shorter (range 2.007(4)−2.083(4), average 2.045 Å) whereas the only $Co-N_{triazole}$ distance is 2.234(3) Å, which is significantly longer.

Magnetic Properties. The tetra- and dinuclear complexes of paramagnetic transition metal ions containing a triazole bridge found in the literature commonly present weak intramolecular antiferromagnetic interactions, mediated by the triazole bridge.[6,7] Not surprisingly, this is also the case of the complexes reported in this work. The magnetic behavior of the cobalt(II) complexes is described below, after the copper(II) and nickel(II) results are discussed (Table 3).

The temperature dependence of the magnetic susceptibility for **1**, **2**, and **4** has been measured between 300 and 1.8 K and is shown as a χT vs T plot in Figure 11. At room temperature, the

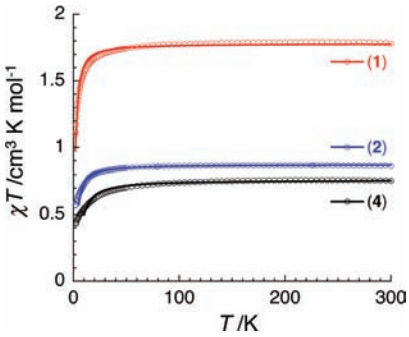

Figure 11. Temperature dependence of χT product (χ being the magnetic susceptibility defined as M/H per complex) measured on a polycrystalline sample of **1**, **2**, and **4** under 1000 Oe. The solid lines represent the best fit described in the text.

χT product is equal to 1.78, 0.86, and 0.75 cm^3 K mol^{-1}, respectively, in good agreement with the presence of four Cu^{II} for complex **1** or two Cu^{II} for complexes **2** and **4**, with $S = 1/2$ and g values slightly above 2. When the temperature is lowered, the χT product at 1000 Oe decreases slightly to reach 1.10, 0.56, and 0.42 cm^3 K mol^{-1} at 1.8 K for **1**, **2**, and **4**, respectively, indicating weak intramolecular antiferromagnetic interactions between Cu(II) spins (Figure 11). On the basis of the physicochemical characterizations (vide supra), complexes **2**

Table 3. Best Set of Magnetic Parameters Estimated from the Temperature Dependence of the Magnetic Susceptibility for 1, 2, 4, 7, and 8

complex	Hamiltonian	J/k_B [K]	g
1	$-2J(S_{Cu1}{\cdot}S_{Cu2})$	−3.4(4)	2.17(5)
2	$-2J(S_{Cu1}{\cdot}S_{Cu2})$	−2.9(4)	2.01(5)
4	$-2J(S_{Cu1}{\cdot}S_{Cu2})$	−5.7(4)	2.15(5)
7	$-2J_1(S_{Ni2}{\cdot}S_{Ni2A}) - 2J_2(S_{Ni1}{\cdot}S_{Ni2} + S_{Ni1A}{\cdot}S_{Ni2A})$	$J_1/k_B = -4.4(2)$, $J_2/k_B = -1.8(2)$	2.12(5)
8	$-2J(S_{Ni1}{\cdot}S_{Ni2})$	−2.2(2)	2.16(5)

dx.doi.org/10.1021/ic202537c | *Inorg. Chem.* 2012, 51, 5058−5069

and **4** can be considered as $S = 1/2$ dimers, while in the case of **1**, such a dimer is decorated by two isolated or very weakly coupled $S = 1/2$ Cu^{II} metal ions (Figure 12 and Table 3).

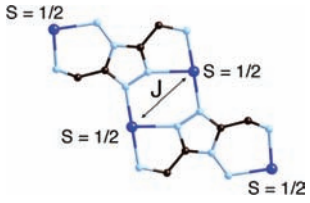

Figure 12. Schematic representation of the spin carriers and their magnetic interactions in complex **1**.

Therefore, the analytical Heisenberg expression of the magnetic susceptibility used to fit the experimental data for **1** is the sum of two $S = 1/2$ Curie laws for the external Cu(II) sites and the magnetic contribution for the Heisenberg $S = 1/2$ dinuclear unit in the low field limit that is given, for example, in ref 45. Whereas the experimental data for **2** and **4** are better described using the susceptibility of a Heisenberg $S = 1/2$ dinuclear unit (see the definition of the magnetic interactions given by the Heisenberg spin Hamiltonians in Table 3). As shown in Figure 11, this model is able to reproduce the experimental data well down to 1.8 K for **1**, to 5 K for **2**, and to 9 K for **4**, with the best set of parameters given in Table 3. As expected, these parameters are in good agreement with those reported for the *dinuclear* complex $[Cu^{II}_2(L^{Tz1})(\mu\text{-}SO_4)](PF_6)_2$ ($J/k_B = -4.3$ K and $g = 2.3$).[19]

The temperature dependence of the magnetic susceptibility for nickel(II) complexes **7** and **8** have been measured between 300 and 1.8 K and is shown as a χT vs T plot in Figure 13.

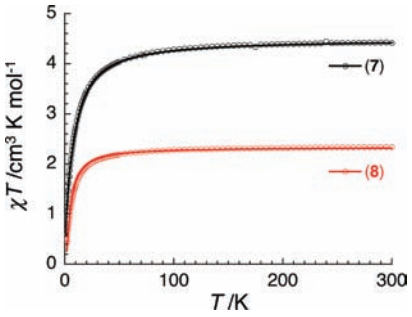

Figure 13. Temperature dependence of χT product (χ being the magnetic susceptibility defined as M/H per complex) measured on a polycrystalline sample of **7** and **8** under 1000 Oe. The solid lines represent the best fit described in the text.

At room temperature, the χT product is equal to 4.4 and 2.3 cm^3 K mol^{-1}, in good agreement with the presence of four and two $S = 1$ Ni^{II} metal ions in **7** and **8**, respectively, and g values slightly above 2. When the temperature is lowered, the χT products at 1000 Oe decrease slowly to reach a value of 0.94 and 0.44 cm^3 K mol^{-1} at 1.8 K, respectively, indicating the presence of intramolecular antiferromagnetic interactions. On the basis of the characterizations reported above, these complexes can be magnetically described as a tetramer and dimer of $S = 1$ ions for **7** and **8**, respectively.

In the case of **8**, application of the van Vleck equation[46] to the Kambe vector coupling scheme[47] allows determination of the analytical expression of the magnetic susceptibility from the following Heisenberg spin Hamiltonian: $H = -2J(S_{Ni1}\cdot S_{Ni2})$. In the weak field approximation, the following definition of the χT product[45] has been used to fit the experimental data:

$$\chi T = \frac{Ng^2\mu_B^2}{k_B}\,\frac{2e^{(2J/k_BT)} + 10e^{(6J/k_BT)}}{1 + 3e^{(2J/k_BT)} + 5e^{(6J/k_BT)}}$$

where J is the intramolecular magnetic interaction between the two nickel magnetic sites. The least-squares fitting of the experimental data down to 1.8 K leads to $J/k_B = -2.2(2)$ K and $g = 2.16(5)$, as presented in Figure 13, confirming the presence of moderated intramolecular antiferromagnetic interactions. These parameters are in good agreement with reported acyclic triazole containing dinuclear nickel(II) complexes found in the literature.[48−51]

In the case of **7**, the susceptibility for the structurally characterized $[Ni_4]$ core was calculated using the following Heisenberg spin Hamiltonian: $H = -2J_1(S_{Ni2}\cdot S_{Ni2A}) -2J_2(S_{Ni1}\cdot S_{Ni2}+S_{Ni1A}\cdot S_{Ni2A})$ where S_{Ni} are the spin operators for each of the metal ions ($S_{Ni,i} = 1$ for Ni^{II} with i = 1, 1A, 2, and 2A, A = $x + 1, -y + 2, -z + 1$). A well behaved simulation down to 1.8 K of the experimental data was obtained using Magpack[52,53] with the following parameters: $J_1/k_B = -4.4(2)$ K, $J_2/k_B = -1.8(2)$ K, and $g = 2.12(5)$, indicating an $S_T = 0$ ground state for this complex (Figures 13 and S22). The magnetic properties of the only structurally characterized complex that presents a similar Ni−(μ-F_2)−Ni motif, $[Ni^{II}_2(L^{MCS})_2(\mu\text{-}F)_2](BF_4)_2$ (Figure S5), also showed antiferromagnetic interactions, with $J_1/k_B = -14.5$ K and $g = 2.17$.[34] Not surprisingly, considering the major differences in the geometrical parameters (vide supra), the coupling constant through the −(μ-F_2) pathway in our *tetranuclear* complex, $[Ni^{II}_4(L^{Tz3})_2(H_2O)_2(\mu\text{-}F_2)](BF_4)_6\cdot 6.5H_2O$, is quite different from that obtained in the *dinuclear* complex $[Ni^{II}_2(L^{MCS})_2(\mu\text{-}F)_2](BF_4)_2$. On the other hand, the coupling constant, J_2, via the triazole bridge for **7** is quite similar to that obtained for our *dinuclear* complex **8** (Table 3).

Magnetic measurements were also performed on microcrystalline samples of the dinuclear Co^{II} complexes: **9**, **11**, **12**, **13**, **14**, and **15**, with an applied magnetic field of 1000 Oe (Figure 14). The χT product at room temperature for these complexes ranges from 3.8 to 4.6 cm^3 K mol^{-1} (3.9, 4.6, 4.2, 4.1, 3.8, 4.1, and 4.5 cm^3 K mol^{-1}, respectively) consistent with the presence of two high-spin Co^{II} metal ions. Indeed, typical Curie constant values for a high spin cobalt(II) metal ion in an octahedral coordination geometry are usually around 2 to 5 cm^3

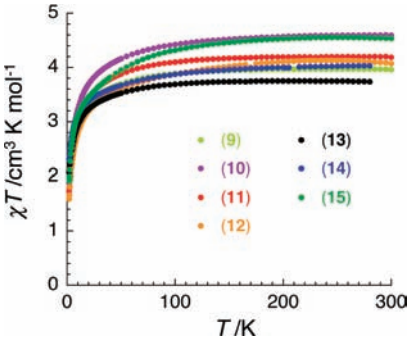

Figure 14. Temperature dependence of χT product (χ being the magnetic susceptibility defined as M/H per complex) measured on polycrystalline samples of **9**−**15** under 1000 Oe.

dx.doi.org/10.1021/ic202537c | Inorg. Chem. 2012, 51, 5058−5069

K/mol depending on the coordination sphere.[54,55] When lowering the temperature, the χT product decreased to a value of 1.80, 1.88, 1.72, 1.59, 2.08, 2.31, and 1.85 cm^3 K mol^{-1} for **9**, **11**, **12**, **13**, **14**, and **15**, respectively. In all of these cases, the decrease in the χT product is generated by the combined effect of intramolecular antiferromagnetic interactions between the metal centers and the intrinsic spin−orbit coupling of the high-spin Co(II) metal ions. The spin orbit coupling results in the splitting of the energy levels arising from the $^4T_{1g}$ ground term, finally stabilizing a doublet ground state.[54] This effect makes the magnetism of these dinuclear systems extremely difficult to analyze in detail and prevent us from modeling the experimental magnetic properties of these cobalt(II) complexes.

CONCLUSIONS

The reactions of the bis-tetradentate triazole-based ligands L^{Tz1}−L^{Tz4} with $M^{II}(BF_4)_2{\cdot}6H_2O$ (M^{II} = Ni, Cu, Co) afforded eight dinuclear and three tetranuclear complexes. When $Co(SCN)_2$ was used as the metal source, three dinuclear complexes were isolated. X-ray crystal structure determinations on eight of these 14 complexes revealed that both di- and tetrametallic complexes had formed, confirming the nuclearity of the complexes obtained indirectly from detailed physicochemical characterizations. These ligands usually bind in a bis-tetradentate manner to two metal ions but can also, when the N^4 substituent is amino, bind in a totally different manner to *three* metal ions to form tetranuclear complexes (e.g., **1**). The other tetranuclear complexes were obtained when the initial, acetonitrile-synthesized, dinuclear products were recrystallized from nitromethane, as F^- ions (presumably from hydrolysis of BF_4 anions) link two such dinuclear complexes together via double fluoride bridges (e.g., **3** and **7**). Hydrolysis of BF_4 anions in alcohol solvents has been well documented in the literature,[22,23] but to the best of our knowledge this is the first time it has been seen in nitromethane (albeit not dried). Two of the dinuclear cobalt(II) tetrafluoroborate complexes, namely, **9′** and **11′**, also featured an unusual bridging tetrafluoroborate anion. This suggests that these compounds could potentially recognize tetrahedral anions, such as phosphates or sulphates, that are important in biological systems.

Relatively strong anion−π−anion "sandwich" interactions, between the central triazole of the ligand and two anions, is a feature seen in seven of the eight structures. In the eighth complex, the central triazole of the ligand is sandwiched by an anion and a solvent molecule. These provide valuable new examples of rarely highlighted anion−π(triazole)−anion/solvent "sandwich" supramolecular interactions.[56−58]

As expected, magnetic measurements show that the triazole and the bis-fluoride bridges mediate intramolecular antiferromagnetic interactions between metal centers leading to singlet spin ground states for the complexes. All of the dinuclear cobalt(II) complexes are stabilized in the [HS−HS] state.

Finally, we have also established the reaction conditions best employed to form dinuclear systems. Armed with this information, it is now possible to attempt the synthesis of neutral iron(II) complexes containing N-based anionic coligands such as NCE (E = S, Se or BH_3), analogous to $[Co^{II}_2(L^{Tz3})(SCN)_4]$. Such iron(II) complexes are usually harder to prepare than other first row transition metal complexes but should show interesting magnetic properties, in particular the spin crossover phenomenon, so these are now being targeted.

EXPERIMENTAL SECTION

General. Solvents and reagents (reagent grade) were purchased from commercial suppliers and used without further purification except for the HPLC grade solvents used in the synthesis of all of the complexes. When specified, complexes were synthesized from dry solvents. Acetonitrile was dried by freshly distilling over calcium hydride before use. Methanol was dried by freshly distilling over magnesium and iodine before use. 3,5-Dichloro-4-amino-4*H*-1,2,4-triazole hydrochloride and 3,5-dichloro-4-(*N*-pyrrol-1-yl)-4*H*-1,2,4-triazole were synthesized according to our literature method.[10] The other 3,5-bis(chloromethyl)-N^4-substituted-1,2,4-4*H*-triazoles were synthesized according to the protocol of Sviridov and co-workers.[21]

For column chromatography, 40−63 μm grade silica gel and chromatography grade neutral aluminum oxide were used. Infrared spectra were recorded over the range 4000−400 cm^{-1} with a Perkin−Elmer Spectrum NBX FT-IR spectrophotometer as a potassium bromide pellet or on a Bruker Alpha FT-ATR with an Alpha-P module. ^{1}H and ^{13}C NMR spectra were recorded on a Varian INOVA-500, INOVA-300, or INOVA-400 NMR spectrometer at 25 °C. ^{1}H NMR assignments were made from 2D-COSY experiments when necessary. ^{13}C NMR spectra were assigned from gHMBC and gHMQC experiments. Elemental analyses were carried out by the Campbell Microanalytical Laboratory at the University of Otago. ESI mass spectra were recorded on a Bruker MicrOTOF$_Q$ spectrometer by Ian Stewart and Matthew G. Cowan (Brooker group).

Magnetic Measurements. Magnetic susceptibility measurements were carried out with a Quantum Design Superconducting Quantum Interference Device (SQUID) magnetometer MPMS-XL housed at the Centre de Recherche Paul Pascal (Bordeaux, France). This magnetometer works between 1.8 and 300 K for dc applied fields ranging from −7 to +7 T. Measurements were performed on microcrystalline samples. The magnetic data were corrected for the sample holder and the diamagnetic contribution of the sample.

X-Ray Crystallography. X-ray data were collected on a Bruker APEX II area detector diffractometer at the University of Otago using graphite-monochromated Mo Ka radiation (λ = 0.71073 Å). The data were corrected for Lorentz and polarization effects, and semiempirical absorption corrections (SCALE) were applied. The structures were solved by direct methods (SHELXS-97) and refined against all F^2 data (SHELXL-97).[59] Unless otherwise stated, all non-H atoms were anisotropically refined. Unless otherwise stated, hydrogen atoms were inserted at calculated positions and rode on the atoms to which they were attached (including isotropic thermal parameters which were equal to 1.2 times to the attached non-hydrogen atom). See the Supporting Information for a detailed description of the commands and disorder models used for each of the complexes. CCDC 846822−846829 contain the supplementary crystallographic data for this paper.

General Synthesis of the Ligands L^{Tz1}−L^{Tz4}. *N*-bis(2-pyridylmethyl)amine (2 equivalents), potassium carbonate (10 equivalents), a catalytic amount of potassium iodide (0.1 equivalents) and 3,5-bis(chloromethyl)-N^4-(substituted)-4*H*-1,2,4-triazole (1 equivalent) were refluxed in 250 mL of HPLC acetonitrile for 20 h and filtered once cool, and the solvent was removed *in vacuo*. The resulting brown red oil was resuspended in 30 mL of water and extracted with dichloromethane (3 × 50 mL). The combined organic phase was dried over $MgSO_4$ and the solvent removed *in vacuo*. The products were obtained as brown oils.

3,5-Bis[bis(2-pyridylmethyl)aminomethyl]-N^4-amino-4*H*-1,2,4-triazole (L^{Tz1}). *N*-bis(2-pyridylmethyl)amine: 1.65 g, 8.31 mmol. K_2CO_3: 2.08 g, 15.08 mmol. KI: 0.07 g, 0.4 mmol. 3,5-bis(chloromethyl)-N^4-amino-4*H*-1,2,4-triazole hydrochloride: 0.82 g, 3.77 mmol. The desired product was isolated in 96% yield, as a brown oil (1.85 g, 3.65 mmol). ^{1}H NMR 300 MHz ($CDCl_3$, $CHCl_3$ @ 7.26 ppm) δ ppm: 3.88 (s, 8H, H5), 3.92 (s, 4H, H4), 7.15 (dt J = 6.45 Hz, J = 6.6 Hz, J = 1.5 Hz, 4H, H9), 7.39 (d J = 7.5 Hz, 4H, H7), 7.61 (dt J = 7.65 Hz, J = 7.8 Hz, J = 1.8 Hz, 4H, H8), 8.51 (d J = 4.8 Hz, 4H, H10). ^{13}C NMR 75 MHz ($CDCl_3$ @ 77.36 ppm) δ ppm: 48.26 (C4), 60.24 (C5), 122.62 (C9), 124.07 (C7), 136.99 (C8), 149.36 (C10), 152.69 (C3), 158.57 (C6). Microanalysis (%) Calcd. for

dx.doi.org/10.1021/ic202537c | Inorg. Chem. 2012, 51, 5058−5069

$C_{28}H_{30}N_{10}\cdot 0.5CH_2Cl_2$: C, 62.34; H, 5.69; N, 25.61. Found: C, 62.40; H, 5.64; N, 23.67. IR (ATR) cm^{-1}: 3245 (br), 3058 (w), 3010 (w), 2925 (w) 2835 (w), 1672 (w), 1589 (s), 1473 (m), 1430 (m), 994 (m), 982 (m), 761 (vs). ESI(+) MS (m/z) MeCN, calcd. for $C_{28}H_{30}N_{10}$: 507.2728. Found: 507.2737.

3,5-Bis[bis(2-pyridylmethyl)aminomethyl]-*N*^{4}-(*N*′-pyrrolyl)-4*H*-1,2,4-triazole (L^{Tz2}). *N*-bis(2-pyridylmethyl)amine: 0.86 g, 4.32 mmol. K_2CO_3: 0.90 g, 6.48 mmol. KI: 0.07 g, 0.4 mmol 3,5-bis(chloromethyl)-*N*^{4}-(*N*′-pyrrolyl)-4*H*-1,2,4-triazole: 0.50 g, 2.16 mmol. The desired product was isolated in 76% yield, as a brown red oil (91.0 mg, 1.63 mmol). ^{1}H NMR 300 MHz ($CDCl_3$, $CHCl_3$ @ 7.26 ppm) δ ppm: 3.69 (s, 4H, H4), 3.82 (s, 8H, H5), 6.17 (t J^1 = 2.1 Hz, 2H, H19), 6.74 (t J^1 = 2.1 Hz, 2H, H18), 7.09 (m, 4H, H9), 7.27 (d J = 8.1 Hz, 4H, H7), 7.54 (dt J^1 = 7.8 Hz, J^2 = 2.1 Hz, 4H, H8), 8.45 (m, 4H, H10). ^{13}C NMR 75 MHz ($CDCl_3$ @ 77.36 ppm) δ ppm: 47.33 (C4), 60.32 (C5), 109.50 (C19), 122.11 (C18), 122.41 (C9), 123.53 (C7), 136.82 (C8), 149.36 (C10), 152.69 (C3), 158.60 (C6). Microanalysis (%) Calcd. for $C_{32}H_{32}N_{10}\cdot 0.5CH_2Cl_2$: C, 63.07; H, 5.42; N, 22.42. Found: C, 62.92; H, 5.53; N, 22.46. IR (KBr) cm^{-1}: 3365 (br), 3103 (m), 2827 (w), 1589 (m), 1569 (m), 1473 (m), 1433 (s), 994 (m), 760 (s),723 (vs). ESI(+) MS (m/z) MeCN, calcd. for $C_{32}H_{32}N_{10}^+$: 557.2884. Found: 557.2889.

3,5-Bis[bis(2-pyridylmethyl)aminomethyl]-*N*^{4}-(phenyl)-4*H*-1,2,4-triazole (L^{Tz3}). *N*-bis(2-pyridylmethyl)amine: 1.75 g, 2.40 mmol. K_2CO_3: 2.37 g, 17.12 mmol. KI: 0.07 g, 0.4 mmol 3,5-bis(chloromethyl)-*N*^{4}-(phenyl)-4*H*-1,2,4-triazole hydrochloride: 1.20 g, 4.20 mmol. The desired product was isolated in 91% yield, as a brown red oil (2.23 g, 3.90 mmol). ^{1}H NMR 300 MHz ($CDCl_3$, $CHCl_3$ @ 7.26 ppm) δ ppm: 3.74 (s, 4H, H4), 3.77 (s, 8H, H5), 7.08 (m, 4H, H9), 7.15 (t J = 9 Hz, 4H, H19 and H20), 7.35 (t, 1H, H21), 7.42−7.52 (m,8H, H8 and H7), 8.44 (m, 4H, H10). ^{13}C NMR 75 MHz ($CDCl_3$ @ 77.36 ppm) δ ppm: 48.28 (C4), 60.17 (C5), 122.28 (C9), 123.48 (C19 and C20), 127.85 (C7), 129.67 and 129.76 (C18 and C21), 136.68 (C8), 149.26 (C10), 153.25 (C3), 158.77 (C6). Microanalysis (%) Calcd. for $C_{34}H_{33}N_9\cdot 0.5CH_2Cl_2$: C, 66.46; H, 5.53; N, 20.10. Found: C, 66.47; H, 5.69; N, 20.15. IR (ATR) cm^{-1}: 3384 (br), 3058 (w), 3054 (w), 2825 (w), 1589 (s), 1569 (m), 1500 (m), 1474 (m), 1433 (s), 1119 (m), 994 (m), 756 (vs). ESI(+) MS (m/z) MeCN, calcd. for $C_{34}H_{33}N_9^+$: 568.2932. Found: 568.2932.

3,5-Bis[bis(2-pyridylmethyl)aminomethyl]-*N*^{4}-(4′-*tert*-butylphenyl)-4*H*-1,2,4-triazole (L^{Tz4}). *N*-bis(2-pyridylmethyl)amine: 0.83 g, 2.50 mmol. K_2CO_3: 2.05 g, 14.82 mmol KI: 0.07 g, 0.4 mmol. 3,5-bis(chloromethyl)-*N*^{4}-(4′-*tert*-butylphenyl)-4*H*-1,2,4-triazole hydrochloride: 0.98 g, 4.90 mmol. The desired product was isolated in 91% yield, as a brown oil (1.4 g, 2.25 mmol). ^{1}H NMR 300 MHz ($CDCl_3$, $CHCl_3$ @ 7.26 ppm) δ ppm: 1.37 (s, 9H, H33), 3.77 (s, 4H, H4), 3.89 (s, 8H, H5), 7.08 (m, 6H, H9 and H20), 7.24 (d (overlap $CHCl_3$), 4H, H7) 7.36 (m, 2H, H19), 7.60 (dt, J = 7.8 and J = 1.8 Hz, 4H, H8) 8.47 (m, 4H, H10). ^{13}C NMR 75 MHz ($CDCl_3$ @ 77.16 ppm) δ ppm: 31.52 (C33), 34.98 (C22), 48.18 (C4), 59.95 (C5), 104.90 (C18), 122.08 (C9), 123.38 (C7), 126.43 (C19), 127.00 (C20) 131.18 (C21), 136.40 (C8), 149.07 (C10), 152.99 (C3).158.76 (C6). Microanalysis (%) Calcd. for $C_{38}H_{41}N_9\cdot CH_2Cl_2$: C, 66.09; H, 6.12; N, 17.79. Found: C, 66.41; H, 6.34; N, 18.50. IR (ATR) cm^{-1}: 3364 (br), 3061 (w), 3009 (m) 2820 (w), 1647 (m), 1590 (s), 1513 (s), 1432 (vs), 1111 (m), 995 (m), 760 (vs). ESI(+) MS (m/z) MeCN, calcd. for $C_{38}H_4N_9Na^+$: 646.3377. Found: 646.3381.

General Synthesis of the Complexes $[M^{II}_2(L^{Tz})(X)_n](BF_4)_m$ (L^{Tz} = L^{Tz1}–L^{Tz4} and M^{II} = Cu, Ni, and Co). Unless otherwise stated, the dinuclear complexes were synthesized as follows: To a solution of the appropriate 3,5-bis[bis(2-pyridylmethyl)aminomethyl]-*N*^{4}-(substituted)-4*H*-1,2,4-triazole (1 equivalent) in the specified volume of acetonitrile, a solution of $M^{II}(BF_4)_2\cdot 6H_2O$ (2 equivalents, M^{II} = Cu, Ni, and Co) in 5 mL of the same solvent was added dropwise. The mixture was stirred for the time indicated. The resulting solution was subjected to diethyl ether vapor diffusion. After the indicated time, the crystalline material was filtered off and dried under vacuum conditions for several hours, or in the case of oils the solution was decanted off and the oil dried for several hours under vacuum conditions, resulting in a solid.

$[Cu^{II}_4(L^{Tz1})_2(H_2O)_2(BF_4)_2](BF_4)_6$ (1). L^{Tz1}: 51.3 mg, 0.10 mmol. $Cu(BF_4)_2\cdot 6H_2O$: 67.73 mg, 0.20 mmol. Stirring time: 3 h. Volume: 30 mL. After 3 weeks, blue crystals suitable for X-ray crystallography were obtained. The solution was decanted, and the solid dried under vacuum conditions, resulting in 34.8 mg of a blue solid (0.023 mmol, 47% yield). Microanalysis (%) Calcd. for $[Cu_4(C_{28}H_{30}N_{10})_2(H_2O)_2](BF_4)_8$: C, 32.80; H, 3.81; N, 14.03. Found: C, 32.59; H, 3.44; N, 13.42. IR (KBr) cm^{-1}: 3425 (br), 2924 (w), 1657 (sh), 1610 (s), 1481 (m), 1443 (s), 1123 (vs), 1083 (vs), 1053 (vs), 770 (s).

$[Cu^{II}_2(L^{Tz2})(H_2O)_4](BF_4)_4$ (2). L^{Tz2}: 50 mg, 0.09 mmol. $Cu(BF_4)_2\cdot 6H_2O$: 60.0 mg, 0.18 mmol. Stirring time: 12 h. Volume: 30 mL. After one week, a blue oil was present. The solution was decanted off, and the oily product was dried under vacuum conditions, resulting in 28.2 mg of a green solid (0.026 mmol, 29% yield). Microanalysis (%) Calcd. for $[Cu_2(C_{32}H_{32}N_{10})(H_2O)_4](BF_4)_4$: C, 36.02; H, 3.40; N, 13.13. Found: C, 36.25; H, 3.43; N, 13.34. IR (KBr disk) cm^{-1}: 3446 (br), 3129 (w), 2923 (w) 1641 (sh), 1611 (s), 1481 (m), 1446 (m), 1314 (w), 1083 (vs), 1051 (vs), 769 (m), 731 (w). ESI(+) MS (m/z) MeCN, calcd. for $[Cu_2(C_{32}H_{32}N_{10})(BF_4)(F_2)]^+$: 807.1401. Found: 807.1011.

$[Cu^{II}_4(L^{Tz3})_2(H_2O)_2(\mu\text{-}F)_2](BF_4)_6\cdot 0.5H_2O$ (3). This complex was synthesized from methanol. L^{Tz3}: 50.0 mg, 0.088 mmol. $Cu(BF_4)_2\cdot 6H_2O$: 58.9 mg, 0.180 mmol. Stirring time: 5 h. Volume: 30 mL. After 1 week, a blue solid was obtained. Microanalysis (%) for this dinuclear sample obtained from methanol, calcd. for $[Cu_2(C_{34}H_{33}N_9)(H_2O)(MeOH)](BF_4)_4$: C, 38.49; H, 3.60; N, 11.54. Found: C, 38.09; H, 4.07; N, 11.46. This blue solid was redissolved in 10 mL of nitromethane and subjected to diethyl ether vapor diffusion. After 1 week, a green solid was obtained. The solvent was decanted off and the green solid dried, resulting in 46.2 mg (0.041 mmol, 23% yield). Microanalysis for this tetranuclear complex, obtained from nitromethane recrystallization (%), calcd. for $[Cu_4(C_{34}H_{33}N_9)_2(H_2O)_2F_2](BF_4)_6\cdot 0.5H_2O$: C, 40.21; H, 3.52; N, 12.41. Found: C, 40.19; H, 3.83; N, 12.52. IR (KBr) cm^{-1}: 3443 (br), 3099 (sh), 2977 (sh), 1657 (w). 1612 (s), 1504 (w), 1161 (sh), 1080 (vs), 1057 (vs), 767 (s), 521 (w). ESI(+) MS (m/z) MeCN, Calcd for $[Cu_2(C_{34}H_{33}N_9)](BF_4)F_3K^+$: 878.1057. Found: 878.1011.

$[Cu^{II}_2(L^{Tz4})(BF_4)_2](BF_4)_2$ (4). L^{Tz4}: 41 mg, 0.065 mmol. $Cu(BF_4)_2\cdot 6H_2O$: 43.94 mg, 0.13 mmol. Stirring time: 5 h. Volume: 30 mL. After 2 weeks, an oil was present. The solution was decanted off and the oil dried under vacuum conditions, obtaining 38.5 mg of a green solid (0.034 mmol, 52% yield). Microanalysis (%) Calcd. for $[Cu_2(C_{38}H_{41}N_9)(BF_4)_4]$: C, 40.24; H, 4.00; N, 11.12. Found: C, 40.51; H, 4.14; N, 11.07. IR (KBr disk) cm^{-1}: 3447 (br), 3123 (m), 2968 (m), 2342 (w), 1623 (m), 1519 (w), 1484 (w) 1449 (m), 1081 (vs), 1058 (vs), 768 (m). ESI(+) MS (m/z) MeCN, calcd for $[Cu_2(C_{36}H_{40}N_{10})(BF_4)_2F_2]Li^+$: 968.2273. Found: 968.2201.

$[Ni^{II}_2(L^{Tz1})(H_2O)_3(CH_3CN)](BF_4)_4\cdot 0.5(CH_3CN)$ (5). L^{Tz1}: 51.0 mg, 0.09 mmol. $Ni(BF_4)_2\cdot 6H_2O$: 62.0 mg, 0.18 mmol. Stirring time: 3 h. Volume: 30 mL. After 3 weeks, pink crystals suitable for X-ray crystallography were obtained. The solution was decanted and the solid dried under vacuum conditions, resulting in 17.6 mg of a brown solid (0.016 mmol, 17% yield). Microanalysis (%) Calcd. for $[Ni_2(C_{28}H_{30}N_{10})(CH_3CN)(H_2O)_3](BF_4)_4\cdot 0.5CH_3CN$: C, 34.26; H, 3.76; N, 15.18. Found: C, 34.44; H, 4.04; N, 14.45. IR (KBr) cm^{-1}: 3462 (br), 1653 (sh), 1609 (s), 1575 (w), 1487 (w), 1448 (m), 1083 (vs), 1059 (vs), 766 (s), 521 (w). ESI(+) MS (m/z) MeCN, Calcd for $Na[Ni_2(C_{28}H_{31}N_{10})](BF_4)_4^+$: 994.1469. Found: 994.2161.

$[Ni_4(L^{Tz3})_2(H_2O)_4(\mu\text{-}F)_2](BF_4)_6\cdot 6.5H_2O$ (7). L^{Tz3}: 108.0 mg, 0.19 mmol. $Ni(BF_4)_2\cdot 6H_2O$: 129.0 mg, 0.38 mmol. Stirring time: 12 h. Volume: 60 mL. After 15 days, a brown oil was present. The solution was decanted and the oil dried under vacuum conditions. Microanalysis (%) for this dinuclear complex synthesized from methanol, calcd. for $[Ni_2(C_{34}H_{33}N_9)(H_2O)_2](BF_4)_4$: C, 38.23; H, 3.49; N, 11.80. Found: C, 38.28; H, 3.92; N, 11.55. It was then redissolved in 10 mL of nitromethane and the light yellow solution subjected to diethylether vapor diffusion. After 1 week, purple crystals were obtained suitable for X-ray crystallography. The crystals were filtered off and dried under vacuum conditions, resulting in 94.7 mg of a gray solid (0.052 mmol, 55% yield). Microanalysis (%) for this tetranuclear complex obtained

dx.doi.org/10.1021/ic202537c | Inorg. Chem. 2012, 51, 5058−5069

from nitromethane recrystallization, calcd. for $[Ni_4(C_{34}H_{33}N_9)_2(H_2O)_4F_2](BF_4)_6{\cdot}6.5H_2O$: C, 38.56; H, 4.14; N, 11.90. Found: C, 38.59; H, 3.86; N, 11.80. IR (ATR) cm^{-1}: 3510 (br), 3065 (br), 1608 (m), 1447 (m), 1287 (w), 1051.36 (vs) 1051.20 (sh), 761 (s), 521 (m). ESI(+) MS (m/z) MeCN, Calcd for $[Ni_2(C_{34}H_{33}N_9)F_3]^+$: 740.1512. Found: 740.1409.

$[Ni^{II}_2(L^{Tz4})(H_2O)_4](BF_4)_4{\cdot}H_2O$ (8). L^{Tz4}: 41 mg, 0.065 mmol. $Ni(BF_4)_2{\cdot}6H_2O$: 44.72 mg, 0.13 mmol. Stirring time: 5 h. Volume: 30 mL. After 2 weeks, the solution was decanted off and the crystals dried under vacuum conditions, obtaining 33.3 mg of a purple solid (0.03 mmol, 46% yield). Microanalysis (%) Calcd. for $[Ni_2(C_{38}H_{41}N_9)(H_2O)_4](BF_4)_4{\cdot}H_2O$: C, 38.73; H, 4.36; N, 10.70. Found: C, 38.52; H, 4.24; N, 10.93. IR (KBr disk) ν cm^{-1}: 3451 (br), 2967 (m), 2328 (w), 1641 (sh), 1610 (m), 132 (w), 1446 (m), 1082 (vs), 1058 (vs), 852 (w), 766 (m). ESI(+) MS (m/z) MeCN, Calcd for $[Ni_2(C_{38}H_{41}N_9)(BF_4)_3]^+$ 1000.2293. Found: 1000.2361.

$[Co^{II}_2(L^{Tz1})(\mu\text{-}BF_4)](BF_4)_3{\cdot}H_2O$ (9). L^{Tz1}: 66.4 mg, 0.13 mmol. $Co(BF_4)_2{\cdot}6H_2O$: 89.30 mg, 0.26 mmol. Stirring time: 12 h. Volume: 40 mL. After 1 week pink crystals suitable for X-ray crystallography were obtained. The solution was decanted off and the solid dried under vacuum, resulting in 31.2 mg of a brown solid (0.032 mmol, 24% yield). Microanalysis (%): Calcd. for $[Co_2(C_{28}H_{30}N_{10})BF_4](BF_4)_3{\cdot}H_2O$: C 33.98, H 3.68, N 14.15. Found: C 34.30, H 3.68, N 13.61. IR (KBr) cm^{-1}: 3445 (s), 1641 (sh), 1613 (m), 1489 (w), 1445 (m), 1127 (sh), 1089 (vs), 1059 (vs), 769 (m). ESI(+) MS (m/z) MeCN: calcd for $[Co_2(C_{28}H_{30}N_{10})](BF_4)_2F^+$ 817.1365 found, 817.1017.

$[Co^{II}_2(L^{Tz2})(\mu\text{-}BF_4)](BF_4)_3{\cdot}2H_2O$ (10). L^{Tz2}: 100.0 mg, 0.18 mmol. $Co(BF_4)_2{\cdot}6H_2O$: 123.0 mg, 0.36 mmol. Stirring time: 12 h. Volume: 60 mL. After one week, pink crystals were present. The solution was decanted off and the crystals dried under vacuum conditions, resulting in 58 mg of a brown solid (0.054 mmol, 30% yield). Microanalysis (%) Calcd. for $[Co_2(C_{32}H_{32}N_{10})(H_2O)_2](BF_4)_2$: C, 36.55; H, 3.45; N, 13.32. Found: C, 36.89; H, 3.45; N, 13.44. IR (KBr disk) cm^{-1}: 3448 (br), 2967 (m), 1613 (s), 1487 (w), 1447 (m), 1270 (w), 1084 (sh), 1057 (vs), 1029 (sh), 849 (w), 771 (s), 521 (w), 417 (w). ESI(+) MS (m/z) MeCN, calcd. For $[Co_2(C_{34}H_{40}N_9)](BF_4)_2^+$: 866.2135. Found: 866.2250.

$[Co^{II}_2(L^{Tz3})(H_2O)_2](BF_4)_4$ (11). L^{Tz3}: 52.60 mg, 0.093 mmol. $Co(BF_4)_2{\cdot}6H_2O$: 63.12 mg, 0.19 mmol. Stirring time: 3 h. Volume: 30 mL. After 15 days, purple solid and brown oil were present. The solution was decanted off and the solid and oil dried under vacuum conditions, obtaining 16 mg of a brown solid (0.015 mmol, 16% yield). Microanalysis (%) Calcd. for $[Co_2(C_{34}H_{33}N_9)(H_2O)_2](BF_4)_4$: C, 38.21; H, 3.49; N, 11.79. Found: C, 38.32; H, 3.46; N, 11.68. IR (KBr) cm^{-1}: 3441 (br), 2923 (sh), 1613 (m), 1480 (w), 1440 (m), 1277 (w), 1084 (sh), 1060 (vs), 1025 (sh), 837 (w), 750 (s), 520 (w).

$[Co^{II}_2(L^{Tz4})(\mu\text{-}BF_4)](BF_4)_3{\cdot}3H_2O$ (12). L^{Tz4}: 90 mg, 0.144 mmol. $Co(BF_4)_2{\cdot}6H_2O$: 98 mg, 0.288 mmol. Stirring time: 12 h. Volume: 60 mL. After one week, pink crystals suitable for X-ray crystallography were present. The solution was decanted off and the crystals dried under vacuum conditions, resulting in 66.3 mg of a brown solid (0.058 mmol, 40% yield). Microanalysis (%) Calcd. for $[Co_2(C_{38}H_{41}N_9)(\mu\text{-}BF_4)](BF_4)_3{\cdot}3H_2O$: C, 39.93; H, 4.14; N, 11.03. Found: C, 39.99; H, 4.13; N, 10.97. IR (KBr disk) cm^{-1}: 3448 (br), 2967 (m), 1613 (s), 1487 (w), 1447 (m), 1270 (w), 1084 (sh), 1057 (vs), 1029 (sh), 849 (w), 771 (s), 521 (w), 417 (w). ESI(+) MS (m/z) MeCN, calcd. for $[Co_2(C_{34}H_{40}N_9)](BF_4)_2^+$: 866.2135. Found: 866.2250.

General Synthesis of the Complexes $[Co^{II}_2(L^{Tz})(SCN)_4]{\cdot}xH_2O$ (L^{Tz} = L^{Tz1}– L^{Tz4}). To a solution of the appropriate 3,5-bis[bis(2-pyridylmethyl)aminomethyl]-N^4-(substituted)-4*H*-1,2,4-triazole (1 equivalent) in the indicated volume of HPLC acetonitrile was added a blue solution of $Co(SCN)_2$ (2 equivalents) in 10 mL of the same solvent. A color change in the solution was observed from blue to dark blue. The solution was stirred for the time indicated below and subjected to diethyl ether vapor diffusion. After the specified time, green-blue solids were obtained and dried for several hours under vacuum conditions.

$[Co^{II}_2(L^{Tz1})(SCN)_4]{\cdot}3H_2O$ (13). L^{Tz1}: 55.0 mg, 0.10 mmol. $Co(SCN)_2$: 38.0 mg, 0.20 mmol. Stirring time: 12 h. Volume: 30 mL. After 1 week, a green solid was present. The solution was decanted off and the solid dried under vacuum conditions, resulting in 18.4 mg of a dark green solid (0.020 mmol, 20% yield). Microanalysis (%) Calcd. for $[Co_2(C_{28}H_{30}N_{10})(SCN)_4]{\cdot}3H_2O$: C, 42.20; H, 3.98; N, 21.53; S, 14.08. Found: C, 41.95; H, 3.19; N, 21.05; S, 14.08. IR (KBr) cm^{-1}: 3446 (br), 2918 (w), 2067 (vs), 1608 (s), 1482 (m), 1437 (m), 1155 (m), 1055 (m), 765 (s), 646 (m). ESI(+) MS (m/z) MeCN, Calcd for $[Co_2(C_{28}H_{30}N_{10})(SCN)_3]^+$: 798.0568. Found: 797.9907.

$[Co^{II}_2(L^{Tz2})(SCN)_4]{\cdot}2H_2O$ (14). L^{Tz2}: 100.0 mg, 0.18 mmol. $Co(SCN)_2$: 62.91, 0.36 mmol. Stirring time: 12 h. Volume: 60 mL. After the stirring time, a small amount of green powder was present, so it was filtered off and discarded. The filtrate was subjected to diethyl ether vapor diffusion. After one week, green crystals were present. The solution was decanted and the solid dried under vacuum conditions, resulting in 99 mg of a green solid (0.111 mmol, 62% yield). Microanalysis (%) Calcd. for $[Co_2(C_{32}H_{32}N_{10})(SCN)_4]{\cdot}2H_2O$: C, 45.86; H, 3.85; N, 20.80; S, 13.60. Found: C, 45.30; H, 3.50; N, 20.92; S, 14.29. IR (KBr disk) cm^{-1}: 3447 (br), 3097 (w), 2917 (w), 2072 (vs), 1604 (s), 1573 (m), 1482 (m), 1439 (s), 769 (s), 738 (s). ESI(+) MS (m/z) MeCN, calcd. for $[Co_2(C_{32}H_{32}N_{10})(SCN)_3]^+$: 848.0795. Found: 848.0724.

$[Co^{II}_2(L^{Tz3})(SCN)_4]{\cdot}H_2O$ (15). L^{Tz3}: 67.0 mg, 0.12 mmol. $Co(SCN)_2$: 41.30 mg, 0.24 mmol. Stirring time: 5 h. Volume: 30 mL. After 1 week, blue-green crystals were present. The solution was decanted off and the crystals dried under vacuum conditions, resulting in 28.8 mg of a green-blue powder (0.033 mmol, 27% yield). Microanalysis (%) Calcd. for $[Co_2(C_{34}H_{33}N_9)(SCN)_4]{\cdot}H_2O$: C, 48.77; H, 3.77; N, 19.46; S, 13.70. Found: C, 48.58; H, 3.69; N, 19.45; S, 13.72. IR (KBr) cm^{-1}: 3447 (br), 2917 (w), 2091 (vs), 2063 (vs), 1602 (s), 1499 (m), 1444 (s), 766 (s). ESI(+) MS (m/z) MeCN, Calcd for $[Co_2(C_{34}H_{33}N_9)(SCN)_3]^+$: 859.0772. Found: 859.0795.

■ ASSOCIATED CONTENT

Ⓢ Supporting Information

X-ray crystallography details and analysis of supramolecular interactions; field dependence of magnetization for complex **7**. This material is available free of charge via the Internet at http://pubs.acs.org.

■ AUTHOR INFORMATION

Corresponding Author

*+64 3 479 7919. Fax: +64 3 479 7906. E-mail: sbrooker@chemistry.otago.ac.nz.

Notes

The authors declare no competing financial interest.

■ ACKNOWLEDGMENTS

This work was supported by grants from the University of Otago, MacDiarmid Institute for Advanced Materials and Nanotechnology (including the award of a PhD scholarship to JO), University of Bordeaux, CNRS, Région Aquitaine, and the GIS Advanced Materials in Aquitaine (COMET Project).

■ REFERENCES

(1) Gavrilova, A. L.; Bosnich, B. *Chem. Rev.* **2004**, *104*, 349−383.
(2) McKee, V. *Adv. Inorg. Chem.* **1993**, *40*, 323−399.
(3) Kahn, O. *Angew. Chem., Int. Ed. Engl.* **1985**, *24*, 834−850.
(4) Klingele, J.; Dechert, S.; Meyer, F. *Coord. Chem. Rev.* **2009**, *253*, 2698−2741.
(5) Olguín, J.; Brooker, S. *Coord. Chem. Rev.* **2011**, *255*, 203−240.
(6) Haasnoot, J. G. *Coord. Chem. Rev.* **2000**, *200−202*, 131−185.
(7) Klingele, M. H.; Brooker, S. *Coord. Chem. Rev.* **2003**, *241*, 119−132.
(8) Kitchen, J. A.; Brooker, S. *Coord. Chem. Rev.* **2008**, *252*, 2072−2092.

(9) Kitchen, J. A.; Noble, A.; Brandt, C. D.; Moubaraki, B.; Murray, K. S.; Brooker, S. *Inorg. Chem.* **2008**, *47*, 9450−9458.
(10) Klingele, M. H.; Moubaraki, B.; Murray, K. S.; Brooker, S. *Chem.—Eur. J.* **2005**, *11*, 6962−6973.
(11) Klingele, M. H.; Moubaraki, B.; Cashion, J. D.; Murray, K. S.; Brooker, S. *Chem. Commun.* **2005**, 987−989.
(12) Grunert, C. M.; Reiman, S.; Spiering, H.; Kitchen, J. A.; Brooker, S.; Gütlich, P. *Angew. Chem., Int. Ed.* **2008**, *47*, 2997−2999.
(13) Bhattacharjee, A.; Ksenofontov, V.; Kitchen, J. A.; White, N. G.; Brooker, S.; Gütlich, P. *Appl. Phys. Lett.* **2008**, *92*, 174104.
(14) Brooker, S.; Plieger, P. G.; Moubaraki, B.; Murray, K. S. *Angew. Chem., Int. Ed.* **1999**, *38*, 408−410 and front cover feature.
(15) Brooker, S.; de Geest, D. J.; Kelly, R. J.; Plieger, P. G.; Moubaraki, B.; Murray, K. S.; Jameson, G. B. *J. Chem. Soc., Dalton Trans.* **2002**, 2080−2087.
(16) Goodwin, H. A. *Top. Curr. Chem.* **2004**, *234*, 23−47.
(17) Hayami, S.; Komatsu, Y.; Shimizu, T.; Kamihata, H.; Lee, Y. H. *Coord. Chem. Rev.* **2011**, *255*, 1981−1990.
(18) Cowan, M. G.; Olguín, J.; Narayanaswamy, S.; Tallon, J. L.; Brooker, S. *J. Am. Chem. Soc.* **2012**, *134*, 2892−2894 and front cover.
(19) Li, D.-D.; Tian, J.-L.; Gu, W.; Liu, X.; Yan, S.-P. *J. Inorg. Biochem.* **2010**, *104*, 171−179.
(20) Lonnon, D. G.; Craig, D. C.; Colbran, S. B. *Inorg. Chim. Acta* **2004**, *357*, 3793−3798.
(21) Ivanova, N. V.; Sviridov, S. I.; Shorshnev, S. V.; Stepanov, A. E. *Synthesis* **2006**, 156−160.
(22) Ackermann, J.; Meyer, F.; Pritzkow, H. *Inorg. Chim. Acta* **2004**, *357*, 3703−3711.
(23) Meyer, F.; Heinze, K.; Nuber, B.; Zsolnai, L. *J. Chem. Soc., Dalton Trans.* **1998**, 207−213.
(24) Lever, A. B. P. *Studies in Physical and Theoretical Chemistry 33: Inorganic Electronic Spectroscopy*, 2nd ed.; Elsevier: Amsterdam, 1997.
(25) Hathaway, B. J.; Billing, D. E. *Coord. Chem. Rev.* **1970**, *5*, 143−207.
(26) Hathaway, B. J. *Struct. Bonding (Berlin)* **1984**, *57*, 55−118.
(27) Addison, A. W.; Rao, T. N.; Reedijk, J.; van Rijn, J.; Vershoor, G. C. *J. Chem. Soc., Dalton Trans.* **1984**, 1349−1356.
(28) Deeney, F. A.; Charles, J. H.; Morgan, G. G.; McKee, V.; Nelson, J.; Teat, S. J.; Clegg, W. *J. Chem. Soc., Dalton Trans.* **1998**, 1837−1843.
(29) Drew, M. G. B.; Harding, C. J.; McKee, V.; Morgan, G. G.; Nelson, J. *J. Chem. Soc., Chem. Commun.* **1995**, 1035−1038.
(30) Guionneau, P.; Brigouleix, C.; Barrans, Y.; Goeta, A. E.; Létard, J.-F.; Howard, J. A. K.; Gaultier, J.; Chasseau, D. *C.R. Acad. Sci., Ser. IIc: Chim.* **2001**, *4*, 161−171.
(31) Allen, F. H.; Bellard, S. A.; Brice, M. D.; Cartwright, B. A.; Doubleday, A.; Higgs, H.; Hummelink, T.; Hummelink-Peters, B. G.; Kennard, O.; Motherwell, W. D. S.; Rodgers, J. R.; Watson, D. G. *Acta Crystallogr., Sect. B* **1979**, *35*, 2331−2339.
(32) Allen, F. H. *Acta Crystallogr., Sect. B* **2002**, *58*, 380−388.
(33) Brezinski, M. M.; Schneider, J.; Radonovich, L. J.; Klabunde, K. J. *Inorg. Chem.* **1989**, *28*, 2414−2419.
(34) Tamayo, A.; Escriche, L.; Lodeiro, C.; Ribas-Ariño, J.; Ribas, J.; Covelo, B.; Casabó, J. *Inorg. Chem.* **2006**, *45*, 7621−7627.
(35) Reger, D. L.; Foley, E. A.; Watson, R. P.; Pellechia, P. J.; Smith, M. D. *Inorg. Chem.* **2009**, *48*, 10658−10669.
(36) Nie, F.-M.; Leibeling, G.; Demeshko, S.; Dechert, S.; Meyer, F. *Eur. J. Inorg. Chem.* **2007**, 1233−1239.
(37) Nie, F.-M.; Demeshko, S.; Fuchs, S.; Dechert, S.; Pruschke, T.; Meyer, F. *Dalton Trans.* **2008**, 3971−3977.
(38) Weller, H.; Siegfried, L.; Neuburger, M.; Zehnder, M.; Kaden, T. A. *Helv. Chim. Acta* **1997**, *80*, 2315−2328.
(39) Nie, F.-M.; Leibeling, G.; Demeshko, S.; Meyer, F. *Inorg. Chim. Acta* **2009**, *362*, 763−770.
(40) Amouri, H.; Mimassi, L.; Rager, M. N.; Mann, B. E.; Guyard-Duhayon, C.; Raehm, L. *Angew. Chem., Int. Ed* **2005**, *44*, 4543−4546.
(41) Meyer, F.; Beyreuther, S.; Heinze, K.; Zsolnai, L. *Chem. Ber.* **1997**, *130*, 605−613.
(42) Zinn, P. J.; Powell, D. R.; Day, V. W.; Hendrich, M. P.; Sorrell, T. N.; Borovik, A. S. *Inorg. Chem.* **2006**, *45*, 3484−3486.
(43) Zinn, P. J.; Sorrell, T. N.; Powell, D. R.; Day, V. W.; Borovik, A. S. *Inorg. Chem.* **2007**, *46*, 10120−10132.
(44) Engelfriet, D. W.; Verschoor, G. C.; den Brinker, W. *Acta Crystallogr., Sect. B* **1980**, *36*, 1554−1560.
(45) O'Connor, C. J. *Prog. Inorg. Chem.* **1982**, *29*, 203.
(46) van Vleck, J. H. *The Theory of Electric and Magnetic Susceptibility*; Oxford University Press: Oxford, U.K., 1932.
(47) Kambe, K. *J. Phys. Soc. Jpn.* **1950**, *5*, 48−51.
(48) Klingele, M. H.; Boyd, P. D. W.; Moubaraki, B.; Murray, K. S.; Brooker, S. *Eur. J. Inorg. Chem.* **2006**, 573−589.
(49) Zhou, J.; Yang, J.; Qi, L.; Shen, X.; Zhu, D. R.; Xu, Y.; Song, Y. *Trans. Met. Chem* **2007**, *32*, 711−715.
(50) Yang, J.; Bao, W.-W.; Ren, X.-M.; Xua, Y.; Shena, X.; Zhua, D.-R. *J. Coord. Chem.* **2009**, *62*, 1809−1816.
(51) Zhou, J.-H.; Cheng, R.-M.; Song, Y.; Li, Y.-Z.; Yu, Z.; Chen, X.-T.; You, X.-Z. *Polyhedron* **2006**, *25*, 2426−2432.
(52) Borrás-Almenar, J. J.; Clemente-Juan, J. M.; Coronado, E.; Tsukerblat, B. S. *Inorg. Chem.* **1999**, *38*, 6081−6088.
(53) Borrás-Almenar, J. J.; Clemente-Juan, J. M.; Coronado, E.; Tsukerblat, B. S. *J. Comput. Chem.* **2001**, *22*, 985−991.
(54) Mabbs, F. E.; Machin, D. J. *Magnetism and Transition Metal Complexes*; Chapman and Hall Ltd.: London, 1973.
(55) Carlin, R. L. *Magnetochemistry*; Springer-Verlag: Berlin, 1986.
(56) Das, A.; Choudhury, S. R.; Estarellas, C.; Dey, B.; Frontera, A.; Hemming, J.; Helliwell, M.; Gamez, P.; Mukhopadhyay, S. *CrystEngComm* **2011**, *13*, 4519−4527.
(57) Robertazzi, A.; Krull, F.; Knapp, E.-W.; Gamez, P. *CrystEngComm* **2011**, *13*, 3293−3300.
(58) White, N. G.; Kitchen, J. A.; Brooker, S. *Eur. J. Inorg. Chem.* **2009**, 1172−1180.
(59) Sheldrick, G. M. *Acta Crystallogr., Sect. A* **2008**, *A64*, 112−122.